Optimization of sustainable, NaCl-resistant and water-repellent renders through evolutionary experimental design

Laura Falchi[a*], Debora Slanzi[a, b], Laura Speri, Irene Poli [a, b], Elisabetta Zendri[a]

[a]Department of Environmental Sciences, Informatics and Statistics, Ca' Foscari University of Venice; Via Torino 155 eta, 30170, Mestre (Venice), Italy; Phone +39 041 2346732; laura.falchi@stud.unive.it; elizen@unive.it;

[b]ECLT, European Centre for Living Technology, Ca' Minich, S. Marco 2940 30124 Venezia, Italy; debora.slanzi@unive.it; irenpoli@unive.it

***Corresponding Author.**
Laura Falchi

Department of Environmental Sciences, Informatics and Statistics, Ca' Foscari University of Venice; Via Torino 155 eta, 30170, Mestre (Venice); Italy

Phone +39 041 2346732

laura.falchi@stud.unive.it

Abstract

The paper deals with the formulation of salt-resistant renders, suitable for the protection of brick masonries subjected to rising damp of salt solution. Natural hydraulic lime, recycled mortars as aggregates, air entraining and/or water-repellent admixtures were selected to produce a double layer render resistant to the action of NaCl solution . The render formulations were optimized by an evolutionary experimental design approach based on Bayesian networks, namely EBN-design, in order to minimize physical damages such as detachments, scaling, efflorescences. Results show that this innovative approach is promising for discovering NaCl-resistant renders by experimentally testing just a limited number out of the possible compositions.

Keywords: Render; Salt Resistance; Recycled Wastes; Evolutionary Design of Experiment; Bayesian Networks; Natural Hydraulic Lime; Water-Repellent admixtures; Air-entraining agents

1. Introduction

1.1 Repairing renders for historical masonries affected by rising damp of marine water

Severe decay of render systems occurs in marine environments due to salty water penetration, salt deposition, sub-efflorescences formation, salt efflorescences, and physical shrinkage occurring at each

crystallization/dissolution cycle [1-8]. Render systems, appropriately calibrated, have demonstrated to tackle the problem by regulating the water flux and salt transport [6-10]. The technical literature describes several renders types developed, studied and applied for the protection and conservation of architectural and historical masonries, among them: traditional renders with slight hydraulic properties or cement composites with high hydraulic properties; slow transporting and water-proof layers or macroporous, highly permeable and sacrificial plasters [6-8].

However, the development of render mixtures durable in marine environments and suitable for historical masonries restoration remains a complex challenge. Several issues have to be taken into account: i) the system effectiveness, in terms of resistance to the disaggregating action of salts, internal cohesion, adhesion to the substrate, external appearance, etc. [9]; ii) the compatibility of the render systems with the historical masonry in chemical-physical terms, as stated in [10-11], iii) the increased awareness regarding eco-sustainability that leads to prefer environmental compatible systems [12-13]. Compatibility and eco-sustainability can be addressed by choosing natural hydraulic lime NHL instead of cement as binder (NHL in fact repeatedly demonstrated a general compatibility with ancient masonries and lower carbon footprint [[12; 14]) and recycled materials as aggregates [15-19]. Effectiveness can be addressed by opportunely testing laboratory specimens, subsequently individuating the most promising systems, optimizing the starting composition to on-field apply and test.

In this study, an evolutionary experimental design approach is presented for the i) evaluation of renders durability when exposed to 3% NaCl solution and the ii) in-lab optimization of render system formulation.

1.2 Optimization of the mixture formulation by experiment design methods

In the traditional approach, owing to his/her expertise, the researcher individuates the suitable starting materials, mix proportions, application and curing conditions, then he/she tests some promising compositions. Since testing all the possible compositions is not economically sustainable, only few compositions are selected: the choice is strictly related to the researcher's experience and previous well-known literature. However, the expert's subjective knowledge on mixture compositions can prevent to select and test promising compositions *a priori* excluded from the experimentation

In the last few years, studies based on statistical designs of the experiments (DoE) and on mixture design modeling are becoming more widespread and offer an alternative approach to the optimization of render formulation.

Through factorial experimental designs, the effects and possible interactions of the different material factors can be assessed (chemical admixtures, mineral additions and water/binder ratio). In k^d factorial designs, a set of possible compositions is defined, where d represent the number of factors (e.g. binders, aggregates, admixtures) and k represents the number of possible levels for each factor (e.g. tot. binder types, tot. different aggregates, tot. different water-repellent percentages) . Analysis of the variance (ANOVA) is then developed on the results of suitable physical properties (e.g. the maximum compressive strength or the capillary water absorption coefficient) to test if any factor produces a statistically different effect on the responses [20-22]. For example, Ribeora et al (2013) [23] evaluated the effect of selected factors such as expanded polystyrene addition content and type and a superplasticizer-water-retaining mix with ANOVA built on a 2^1x4^1 mixed-level full factorial design on capillary absorption and compressive strength, whereas Ferrandiz et al (2016) [24] proposed a 3^3x2^1 d-optimal experimental design to evaluate the effect of incorporation of recycled glass fibre reinforced plastics on the mechanical behaviour of polyester polymer mortars. These DoE approaches generally requires to experimentally test almost all or even all the possible combinations; therefore they are suitable when a very limited number of factors and/or levels of factors are investigated. Moreover, to develop analysis on the effect of the factors or interactions amongst factors, simple models with a small set of interactions are usually assumed.

While the number of variables and their different nature, as well as the limited number of points that can be tested due to technical and economical constraints, can make it very difficult to use classical DoE methodologies, planning efficient and effective experiments is essential to achieve good results in such areas of research where experimentation is complex, extremely expensive and time consuming.

In this study, an innovative approach based on evolutionary experimental designs is proposed: the Design of Evolutionary Experiments based on Models approach (DEEM approach) [25-28]. DEEM approach has been recently developed to derive small sets of informative experimental points (i.e. to experimentally test a limited number of compositions), when classical hypotheses of statistical designs and multidimensional modelling are missing.

The design, consisting of a collection of experimental points, is regarded as a population that evolves across generations according to the evolutionary paradigm. Each population of experiments is very small with respect to the size of the possible designs (i.e. all the possible combinations according to the variables and their levels), but it changes throughout generations, "learning" from one generation to the next and exploring, in an intelligent way, the search space.

Statistical models are used to identify the relevant information at each generation and this information is incorporated in the evolutionary procedure, making the search more efficient and effective. In particular, our approach is based on the evolution of Probabilistic Graphical Models, PGMs [29-31], i.e. models where a graph-based representation is combined with the rules of probability theory to provide a flexible framework for modeling large collections of variables with complex interactions. We focus on a particular class of PGMs, that is the class of Bayesian network models (BNs), where the graph representation is based on nodes corresponding to random variables and on arcs between nodes, describing the probabilistic dependence structure that may characterize the set of variables on which we then develop statistical inference [32-33].

When a limited number of experimental points, i.e. promising compositions, can be tested due to technical and economical constraints, the information achieved by statistical models is adopted to guide the optimization towards the objective of the experiment. The "optimal composition" can be defined in relation to specific environmental situations and to desirable properties, allowing a good durability and compatibility.

DEEM approach is very flexible, since it can be developed using different classes of models and with different evolutionary procedures. Moreover it has the great advantage of significantly limiting the experimental tests (in our case just 30% of the possible combinations were experimentally tested) and it has been proved to produce very successful results in a large set of experimental studies [26-28; 34-35].

1.3 Aims and structure of the work

In this study, the specific aims were:

- to individuate render multilayer systems able to resist to rising damp of 3% NaCl solution and to minimize the degradation patterns such as detachments, disaggregation, sub- and efflorescence formation;

- the individuation of the promising systems within a large and complex set of possible compositions by applying DEEM approach based on Evolutionary Bayesian Network models, in order to avoid *a priori* and subjective decision of few testable mixtures;
- to highlights strengths and weaknesses of this approach when applied to the development of complex render systems.

Double layer render systems on bricks specimens, based on natural hydraulic lime NHLas binder and recycled crushed mortars were considered. Moreover, air-entraining agents, water repellent admixtures, different water binder ratios, were taken into account in order to act on porosity and wettability which are usually related to the salt- resistance, as highlighted in previous researches [2-7, 36-40]

The systems, produced according to the indication of the experimental design, underwent cycles of capillary absorption of 3% NaCl solution and drying cycles to simulate the effect of marine water.

Subsequently, visual observation, weight variations, the capability to remain adherent to the brick under mechanical solicitation and salt distribution were assessed. Based on the results and on an expert elicitation [41-42] four detrimental effects, i.e. the presence of detachments, internal de-cohesion and crumbling, external erosion/exfoliation and external efflorescences, were identified as response variables Y_i and evaluated with a mark. This mark, chosen in a 10-point scale ranging from 1 to 10, was assigned to each detrimental effect and considered as observed value of the associated response variable.. Then a statistical model built for both response variable and design variables were estimated from the available data. The successive generation of experiments was therefore determined by predicting the estimated behaviour of the system variables by means of the information achieved from the statistical model. The process was repeated three times in order to minimize the degradation effects and optimize the system behaviour.

Following the evolutionary characteristic of the proposed approach, in this paper we present the results obtained for each tested generation, and finally the model achieved at the end of the process is presented and discussed.

2. Materials and Methods

2.1 Starting Materials and design variables

Table 1 summarizes the brick substrate, the double layer render system and its general composition.

In order to resemble a traditional masonry, full, red-fired bricks (by San Marco Laterizi S.p.A., dimensions 16cm X 12cm X 2cm) were chosen as substrate for the render application.

The preparation of the first layer of render involved the following starting materials: natural hydraulic lime NHL 3.5 supplied by MGN as binder; limestone- siliceous sand with a size fraction of 0/5 mm as aggregate; recycled aggregates (size fraction 0/5, Boloomey distribution, obtained by crushing old water-repellent mortars made of limestone cement, natural hydraulic lime and pozzolana-lime [38; 40]); sodium alkyl sulfonate admixture as air entraining agent; tap water used in two different water–binder proportions.

For the preparation of the second layer NHL 3.5, a limestone- siliceous sand (size fraction 0/2 mm) and water repellent admixtures (calcium stearate by SIGMA Aldrich or the powdery siloxane product Sitren P750 by Evonik) were employed.

.In order to design optimal renders with respect to specific properties, we defined the set of design variables $\mathbf{X}=(X_1,X_2,X_3,X_4)$, where each X_i represents a particular component of the specimen (Table 1):

- X_1: Recycled aggregate, assuming the set of possible values x_1={CM, CM750,CMcast, PM, PM750, PMcast, NM, NM750, NMcast}
- X_2: water/binder ration, assuming the set of possible values x_2={1.0, 1.2}. These levels were chosen in order to obtain to obtain either a regular mixture workability, either a fluid mixture with a final higher porosity [43-44]
- X_3: % of air entraining, assuming the set of possible values x_3={0.03, 0.09}. The three possible ratios were chosen for the air entraining agents in order to obtain different microstructures and porosity, in particular the second ratio is a percentage commonly used in dry-mix products, whilst the third is able to obtain a macroporous structure [45-46]
- X_4: % of water repellant, assuming the set of possible values x_4={0, 0.03, 0.05}. These ratios are commonly used in commercial products and in previous researches [36, 38, 47].

Under this setting the whole combinatorial search space Ω consists of 9*2*2*3=108 possible specimens types (experimental points). Applying DEEM approach based on Evolutionary Bayesian Network, EBN-design, we limit the number of candidate experimental points to 28 representing just the 26% of the tests to be conducted. Since each experimental point corresponds to three replicated specimens, 84 specimens were physically produced out of 324 theoretical specimens.

2.2 Specimens preparation and exposure

The composition of each specimen was indicated by EBN-design in each generation of the procedure (see also paragraph 2.4), whilst their preparation and exposure is based on the Protocol proposed within the COMPASS project [8]. The choice of the testing protocol is particularly difficult when the resistance to salt degradation of multicomposite systems is considered, since no precise normative is available [48], the COMPASS protocol was chosen since it demonstrated to be particularly suitable in highlighting salt-induced degradation. Mock-ups made of full, fired clay bricks, covered by a double layer of render were prepared (Figure 1). The preparation of the first layer involved mixing of the binder with half the water and with the air entraining agent at a low speed (100 rpm) for 5 minutes, then the remaining water and the aggregates were incorporated and mixed for a further 5 minutes. The mixture was then applied on moist bricks to form a layer 1 cm thick and patting the surface with a trowel in order to enhance the adhesion of the second layer. The specimens were cured for 12 hours at 95% HR and 20°C before the application of the second layer. The second layer, 0.5 cm thick, was prepared by applying the mixture of binder, water, aggregates and water repellent admixtures (when present) on the first layer, then smoothing the surface with a trowel. The specimens were cured in environmental atmosphere at 95% HR and 20°C for 28 days, then dried at room temperature till constant weight (HR% 55%, T 23 °C). Three independent replicates were prepared for each experimental point. The major differences with the COMPASS protocol are the larger dimension of the specimens (16cm x12cm x2cm) and the absence of lateral sealing, in order to enhance mocks-up representativeness.

Once hardened, each system was subjected to drying-wetting cycles by capillary rise of 3% by weight NaCl solution, in order to simulate the salinity of the sea water. The bottoms of the specimens were immersed in the salt solution for 24 hours to ensure complete wetness also in the presence of water repellent admixtures. The specimens were then removed from the container and placed at HR 65%, T23°C for a 7 day drying, thus avoiding excessive stress on the material and allowing the evaporation of 80% of the solution before the following cycle. Four cycles were performed in one month of exposure without removing efflorescence or debris from the surface of the specimens at each cycle.

2.3 Evaluation methods

In order to highlight the resistance to salt crystallization cycles, the specimens were weighted at each cycle, while photographic documentation and 1200dpi scans of the surfaces by a Epson perfection 3170 Photo was taken after the cycles to record the presence of decay forms such as efflorescences, cracks, erosions linked to the extension of stains, crusts and eroded areas. The visual damage was revealed also by optical microscopy observations with a DINO-lite Premier AM4113T microscopy (10-200x), 1.3 MPx. Moreover, colorimetric measurements were performed using a CM2600d Konica Minolta portable spectrophotometer with aD65 illuminant and 10° standard observer to quantify the SCI (Specular component included) colour variations due to erosion or salt crusts formation [49]. In order to consider the high surface inhomogeneities and obtain a repeatable measure, a medium averaged spot size of 8 mm Ø, an average of 5 points with 3 scans each was considered for each specimen. The formation of salts crusts and efflorescences on the surfaces lead to more or less extended white stains with lightness increase over 5 points, the formation of sub-efflorescences lead to delamination and erosion of the surfaces with lightness decrease over 5 points.

In order to evaluate the internal degradation and possible detachment of the render layers enhanced by salt crystallization, a Schmidt Pendulum Hammer PT sclerometer for soft materials was used. The instrument measures the rebound of a spring loaded mass impacting against the surface of the sample., The mass is constituted of a cylindrical hammer head of 40mm diameter and 720g that slides on an arch, the hammer head can be loaded in fixed position, then released in order to impact the surface with an impact energy of 0,83Nm or 0,44J [50] . The strokes give a reproducible mechanical solicitation that might cause detachment or failure of degraded layers and the rebound is dependent to the hardness of the material (tabulated in specific graphs by the instrument producer). Five hammer strokes at percussion energy 0.44J were followed by other five at 0.83J, by choosing a different starting angle of the pendulum. The specimens that endure all the strokes without failures or detachments demonstrated optimal cohesion and salt resistance, moreover, the higher the rebound, the stronger the internal render cohesion.

The salt distribution profile at the end of the test was used as an indication of salt transport within the plasters and the possibility to sub-surface damage. The renders were cut without the use of water in 4slices, and the conductivity was determined according to NorMaL 13/83 with the EC-meter GLP31 by Crison [51].

To evaluate the quality of each candidate point, i.e. the overall resistance of each system to salt decay, four parameters of decay (i.e. response variable Y_i, i=1,..,4) were selected and evaluated by using the results of the observations and measurements and by elicitation of the researcher. In order to guarantee an opportune of elicitation, the researcher should have sufficient background experience to autonomously identify the typical degradation patterns, the properties and behaviour of render systems suitable for historic masonries. The parameters, selected for their severity and representativeness, are:

- Y_1=presence of detachments and cracks formation (the behavior after the mechanical solicitation with Schimdt Hammer is considered, together with visual observation of cracks);
- Y_2=internal de-cohesion and crumbling (hardness and elastic properties measured by the hammer rebound is considered together with mass losses and visual observation);
- Y_3=external erosion/exfoliation (visual observation, erosion extent, colorimetric measurements and position of salts by conductivity measurement are taken into account);
- Y_4=external efflorescences (white stains and crusts extent and colour variation are considered).

Each response variable is evaluated with a mark from 1 to 10, where 1= non present; 10= completely present, e.g. Y_1= 10 if complete detachment of the render layer from the substrate occurs without hammer strokes or with low energy strokes (0,44J), Y_1=1 if no detachment occur after 10 strokes; Y_2=8-10 if negative mass losses ($\Delta M\% \leq -2$) and low rebounds (≤ 8) are measured; $Y_{3,4}$= 10 if the degradation extent cover the whole surfaces, $Y_{3,4}$ =1 if it covers less than 20% of the surface. The averaged results of the three replicates for each experimental point is considered.

We can then assume that these decay forms have decreasing importance; in fact the render and the masonry undergo severe damage if the render is completely detached or if its internal cohesion is scarce due to salt action; external exfoliation and erosion cause surface damage limited to the render; external efflorescences do not physically damage the masonry or render, but might induce prolonged render wetness due to salt hygroscopicity and aestethical damage. Therefore, in order to define a unique response function Y to optimize, we will introduce a weighted combination of the selected parameters defined as $Y=0.4Y_1+0.3Y_2+0.2Y_3+0.1Y_4$.

2.*4 DEEM approach based on Evolutionary Bayesian Networks (EBN-design)*

The DEEM approach based on Evolutionary Bayesian Networks, EBN-design, begins by randomly generating a first population of n_1 experimental points $\mathbf{X}_{n1}=(\mathbf{x}_1\ \mathbf{x}_2\ldots\mathbf{x}_{n1})$, where each point $\mathbf{x}_k=(x_{k,1}x_{k,2}x_{3,k}x_{k,4})\in\Omega$, k=1,…, n_1, represents the particular combination of components producing a specific specimen.

This initial design is then prepared and tested as described in paragraph 2.2. The degradation patterns were evaluated as described in Paragraph 2.3 thus providing the first set of response values, namely the vector y_{n1}. At the end of this step the set of data $D_1=(\mathbf{X}_{n1},\ \mathbf{y}_{n1})$ representing both the tested specimens and their corresponding observed responses, is available for the first generation.

This set of data is modeled by a Bayesian network models, which is formally represented by a directed acyclic graph (DAG) and a probability distribution (P). DAG represents the structure of the BN and it is composed of nodes representing the set of random variables $X=(X_1,X_2,...,X_d)$, each of which can take a value in a finite set of possible mutually exclusive variable values, and of arcs between nodes in the form of $X_i\rightarrow X_j$, indicating direct probabilistic dependencies between the corresponding variables. The correspondence between the structure of the DAG and the dependence and independence relationships among the variables is derived by the d-separation criterion [31-32]. This criterion in fact uses the properties of the path structures and graph theory to define whether two nodes are independent conditioned to another node or set of nodes. Then from the identification of the dependence/independence relationships, the Markov property is assumed stating that there are no direct dependencies in the system being modeled which are not already explicitly shown via arcs and d-separation [31-32]. Finally by means of the Markov property, the joint probability distribution P can be written as in the following factorization:

$$P(\mathrm{X}=\mathrm{x})=\prod_{i=1}^{n}P(X_i=x_i\left|Pa(x_i)\right.)\qquad \mathrm{i}=1,\ldots,\mathrm{d}\quad(1)$$

where $\mathbf{X}=\mathbf{x}$ indicates that the set of variables $\mathbf{X}=(X_1,X_2,...X_d)$ is observed at specific values $\mathbf{x}=(x_1, x_2, \ldots x_d)$, and $Pa(x_i)$ is regarded as the particular value realization of the parent set of X_i, i.e. all the variables with a direct arc to X_i. The set of conditional probabilities $P(X_i=x_i|Pa(x_i))$, i=1,...,d, represents the set of parameters of the Bayesian network. The simplification of the joint probability distribution given b Eq.1 allows complex

systems to be analyzed and modeled using a limited number of local relationships and to be regarded as stochastic models, built up by combining together simple components.

When a particular target variable Y, i.e. class variable, is identified within the set of variables, we can see the Bayesian network as a probabilistic classifier [32, 52]. These classifiers are used in many applications as they are able to probabilistically identify to which target value a new observation belongs based on the observation of the values assumed by the other variables of the system. In particular, Bayesian classifiers such as Naive Bayes [53] or Tree Augmented Naive Bayes, TAN [54-55] are graphical models composed of nodes and arcs among nodes with particular structures. Naïve Bayes assumes that the target variable Y has a direct dependence relationship with all the X_i variable of the system, $Y \rightarrow X_i$, but no dependencies are admitted among the set of X_i; TAN relaxes this assumption assuming that the target variable Y has no parents and each variable X_i has as parents the target variable and at most one other variable X_j. In this research we will focus on TAN classifiers as they are a restricted family of Bayesian networks and they are proven to perform very well in chemoinformatics applications [52].

Following EBN-design we built a TAN classifier and used the achieved joint probability distribution to predict the estimated values $\hat{y}_{1,\Omega}$ of the class variable for all the possible points of the search space. From the set of values $(\Omega,\hat{y}_{1,\Omega})$ we select the sub-set of n_2 experimental points with optimal predicted class values. This new set of points $\mathbf{X}_{n2}=(\mathbf{x}_1\,\mathbf{x}_2 \ldots \mathbf{x}_{n2})$ becomes the second population of the evolutionary procedure and is evaluated yielding the new data $D_2=(\mathbf{X}_{n2}, \mathbf{y}_{n2})$.

This process is iteratively repeated, generation after generation, and ends when total number of experimental points is tested. In particular in this experimentation we build EBN-design selecting a population of $n_q=7$ specimens and evolving the algorithm through 3 generations, i.e. q=1,2,3. Only for the first generation, as we need to test all the recycled aggregates (the 9 possible values of variable X_1), we randomly select 14 candidate experimental points by assuming that all the aggregates were selected almost once. With this design setting, we then evaluate only 28 possible candidate specimens representing 26% of the whole search space. EBN-design and all the statistical analysis were performed using the R statistical software [56]

3. Results

Table 2 reports the mixture compositions of the specimen population defined in the three generations. The three generations were prepared and tested separately and subsequently, since the results of each generation was used to estimate a model of the experimental space and to indicate the optimized mixtures for the next generation. Therefore, the discussion is presented by highlighting the results of each sequential generation.

3.1 First generation

After 28 days of maturing, some of the render layers detached bodily from the bricks, even before the crystallization cycles, as indicated in table 3 and shown in Figure 2. Y_1 (detachments) was evaluated as 10 when bodily detachment occurs before the exposure.

Besides the detached specimens, the more recurrent decay features were (Figure 2): slight presence of efflorescences without substantial loss of material and slight darkening of the surface for the series 1.7 and 1.1; diffuse presence of efflorescence (1.2,1.3, 1.4, 1.11); spalling and surface delamination (1.13, 1.14,1.5); diffuse delamination and complete detachment from the surface layer (1.6, 1.8, 1.9, 1.10). The variations of colour components a* and b* are negligible, whilst ΔL^* and the total variation ΔE are almost coincident. The prevailing colour of the mortars is gray and the salts can cause white efflorescences or a darkening effect (hue saturation) due to surface erosion or hygroscopic humidity retention(Figure 3).. The series 1.5,1.4,1.2, 1.10 were affected by a higher absolute colour variation, with darkening mainly due to loss of the external layer in the case of 1.5, 1.10 and to hygroscopic humidity for 1.4 and 1.2.

The weight variations seem to reflect the appearance of the specimens (Figure 4): weight variation of series 1.1 to 1.6 is not significant and a lesser presence of salt crusts and efflorescences were observed, while positive weight variation were observed for the series 1.10, 1.11, 1.13, 1.14 due to salt accumulation within and over the specimens, evident also by visual observation. The differences at each cycle could be due to a different drying behavior of specimens more polluted by salts.

Before the exposure, the different series showed similar conductivity of around 42±10 μs/cm in the internal layer and 70±20 μs/cm in the external layer. After the exposure, the conductivity profiles (Table 3) indicate that most of the specimens accumulate salts close to the surface, pointing out the presence of efflorescences or subefflorescences. In particular, the series 1.1, 1.3 maintained high salt concentration in the whole profile;

1.7 and 1.11 (with 0.5% and 0.3% of water repellent on the external layer) shown salt accumulation behind the surface; 1.2 maintained a uniform increasing profile; 1.8 (without water repellent admixture) showed a lower conductivity in the middle layers.

Hammer rebound test (table 3) highlighted that series 1.3, 1.6, 1.14, 1.10, did not detach before the salt cycles and were able to endure 7 strokes before bodily detachment, even if the mean hammer rebounds values were around 10, denoting soft mortar layers. 1.9 and 1.13 also demonstrated an acceptable adhesion before the cycle (1 specimen over 3 detached by themselves) and after the cycles, by enduring at least 9 strokes. In every case, high standard deviation were calculated, due to the intrinsic heterogeneity of the systems, which caused rebound variation within each specimen.

Based on the observed behaviour, in particular on the absence/presence and extent of the different degradation pattern Y_i, the marks assigned to the specimens of Generation 1 are reported in Table 4 (rows 1-14).

3.2 Second generation.

Table 2, rows 15-21, reports the mixture compositions (2.1-2.7) of the population provided for the second generation from the information achieved by TAN model estimated for the response variable Y, i.e. the mark of the specimens, and design variables, i.e. specimen components.

After 28 days of curing and the first drying, the render layers of set 2.3, 2.4, 2.5 detached bodily from the bricks, pointing out a lack of flexibility and an insufficient adhesion (Table 3).

The exposure caused recurring patterns within each set of specimens (Figure 2), in particular: 2.2 was the unique set showing scarce crumbling and few salt efflorescences on the surfaces, whilst 2.4 and 2.5 specimens were covered by salt efflorescences, serious erosion of entire surface areas occurred. The colorimetric measurements shown in Figure 5 agree with the visual observation, denoting a lightness ΔL^* and total colour ΔE variations were higher than the first generation, in particular for 2.4 and 2.2.

The salt accumulation within and over the specimens caused a common increasing trend regarding weight variation during the cycles (Figure 6). Weight discrepancies were observed particularly after the first cycle, possibly due to a higher salt transport and accumulation, without crumbling or material losses, in comparison to the following cycles. Then, spalling and crumbling occurred with loss of material, counterbalancing the

salt accumulation and efflorescence formation. The relative variation amongst the different sets could be due to different presence of salts in relation to the water repellent behavior, the pore structure and the hygroscopicity of the systems.

Also for the second generation, the conductivity measurements indicate (table 3) a higher salt concentration in the external parts of the systems in comparison to internal parts, due to deposition of salt on the surfaces. However, 2.1, 2.2 and 2.6 had high concentration also nearby the brick.

In comparison to the first generation, the different series endured higher mechanical solicitation with at least 9 strikes before bodily detachment. In particular, 2.4 and 2.6 demonstrated optimal adhesion even after repeated strikes and rebounds over 20°, denoting a coherent, but still elastic structure.

Marks assigned to the specimens of Generation 2 are reported in Table 4 (rows 15-21).

3.3 Third generation

The mixture compositions defined in the third generation, achieved by modeling marks of the first and second generation, are presented in table 2, rows 22-28.

In this generation just one specimen underwent bodily detachment from the brick before the exposure. After the cycles, decay patterns such as crumbling and spalling were limited in comparison to previous generations (Figure 2). However, salt crusts and salt efflorescence formation were observed for several series. Colour variations exceeding 5 points of ΔL^* or ΔE were observed for 3.7, 3.4 and 3.1 series, due to surface loss of material and presence of efflorescence (Figure 7).

The weight variation showed trends similar to the second generation, due to salt accumulation and humidity retention due to salt hygroscopicity (Figure 8). In particular 3.1a and 3.1b, 3.5, 3.6 showed loss of material and thick salt crust formation. However, only the conductivity profile of 3.6 (table 3) indicates a higher salt concentration in the external render layer, whilst 3.1 and 3.5 showed quite homogenous profiles. It is possible that a quick salt transport mechanism with deposition of salt only occurred on the external surface. 3.2 and 3.7 series had high conductivity in the 10-12 mm range corresponding to the subsurface part, thus indicating storage of salt crystals within the specimens. 3.4 showed an increasing trend of conductivity values from the internal part to the surface.

Reduced detachments/delamination were observed under mechanical solicitation by Schmidt Hammer after the cycles (Table 3). 3.2 and 3.7 were more stiff in comparison to the other series, with hammer rebounds higher than 30° for impact stress of 0.88J, possibly also due to the formation of rigid subsurface salt deposition (indicated by conductivity profiles). Values over 20° for impact stress of 0.88J were measured for the other specimens, demonstrating a good balance among stiffness and compactness.

Table 4 reports the evaluation of the specimens composing the third generation, rows 22-28.

4. Discussion

4.1 Evolution of the EBN-design across generations and minimization of the degradation features

The evaluations carried out for each generation have allowed us to investigate and model the experimental space. In Figure 9, the evolution of the EBN-design across generations is presented, in particular Figure 9a show the evolution of the mean response function Y and its corresponding standard error . Notably, the mean response decreased from Y=5.03 (sd=2.3) to Y=3.09 (sd=0.87), corresponding to lower decay features and a 38% improvement, just in 3 generations of the process. The same behaviour can be observed considering Y_1 (detachments) and Y_2 (internal de-cohesion) response variables (Figure 9b), which are the decay features that can cause complete failure of render systems and are responsible for the 40% and 30% respectively of Y, as described in Section 2.2.1. Y_3 (external exfoliations) and in particular Y_4 (efflorescences) usually cause aesthetical damage and not structural collapse, therefore contribute less to the definition of the response function Y and their behaviour reveals this characteristic. In particular in the 3^{th} generation, a homogenous transport of salt solutions to the surface is often observed and the evaporation of water from the external surface leads to crystallization of the salts as innocuous salt efflorescence, avoiding spalling [6-8].

Considering all the experimental points ordered by generations, as presented in Figure 10, we can see how the variability of the response decreases. In the first generation, we selected a random sample from the possible specimens, achieving responses with a wide range of values, some of them with response value Y smaller than 3 (4 specimens out of 14, i.e. 28% of the experiments in generation 1). After just 2 generations of the process, we significantly reduced the range of response values in the interval [1.67, 4.32] with 3 specimens having response value Y smaller than 3 (i.e. 43% of the experiments in generation 3).

421 Given that our aim was to derive a very small set of informative experimental points with respect to the
422 whole search space, these results seem very good as the EBN-design has a high probability to improve the
423 sustainability and resistance of the renders in the early generations of the design, saving experimental
424 resources and reducing possible waste. Moreover, the approach achieved good values testing just a small set
425 of the whole experimental space, namely less than 26% of the candidate experimental points.
426
427 *4.2 The TAN model after three generations: the probabilistic influence of the composition on the resistance*
428 *to NaCl exposure*
429 The results obtained during the experimentation were used to estimate a TAN model at the end of each
430 generation of the EBN-design process. The TAN model estimated at generation 3 derived by all the tested
431 data of this experimentation, i.e. at the end of the evolutionary procedure, is presented in Figure 11. The class
432 variable represents the target of the optimisation, i.e. the response variable Y, which describes the degree of
433 decay occurred. As required by TAN models, each design variable (recycled aggregate, w/b ratio, water
434 repellent percentage and air entraining percentage) has Y and at most one variable as parents, as indicated by
435 the direct arcs in the network . In this way, we are able to identify the strongest relations amongst the design
436 variables X_i, i=1,…4, with the detrimental effect Y, and how the interconnection network amongst them is
437 developed.
438 It is notable that the type of recycled aggregate is a key factor in the experimentation, as the corresponding
439 variable is parent of all the other variables in the network. This implies that when choosing a specific
440 aggregate, the value of the percentage of water repellent, the water/binder ratio and the percentage of air
441 entraining follow from that assumption. The aggregate type is therefore a significant variable and this needs
442 to be taken into account when using recycled aggregates. In particular, the presence of recycled mortars
443 which are internally water-repellent may have a direct effect on the water transport properties of the first
444 layer, hindering the moisture transport and favouring salt deposition at the interface substrate-first layer, in
445 particular for cement based aggregates (e.g. for mixtures 1.10, 1,11 that had as aggregates CM750 and
446 CMCast containing in turn a 0.5% of water-repellent agent). Whilst the presence of pozzolana or of NHL
447 aggregates may lead to side reactions of the binder, favouring the formation of hydration products and
448 enhancing the strength (e.g. mixtures 1.3, 1.5, 3.2, 3.1 that contains the aggregates PM, NM, NMcast). The

449 effect of the recycled aggregate on the final structure and behaviour, needs to be compensated by the
450 adequate choice of additives and additive dosages, in order to obtain a good durability in the presence of
451 rising damp of salt solutions.
452 When TAN is estimated, we can develop probabilistic inference about design variables, deriving in this way
453 the strength of the relationships among each variable and the decay represented by Y. For example, given
454 that we observed a very low value of Y, say for example included in the interval [1,2), we will derive a
455 probability equal to 0.332 that a specimen is composed by CMcast aggregate. Moreover, conditioned to very
456 low value of Y, the probability of selecting specimens with a water/binder ratio of 1.0 and 1.2 is 0.532 and
457 0.522 respectively, showing that these w/b ratios are equally probable, whilst the aggregate type is not. This
458 confirms the hypothesis that the interconnection network has a key variable in the type of aggregate. In fact,
459 if we condition to a very low value of Y and a CMcast aggregate, we observe with probability equal to 0.896
460 a specimen with water/binder ratio of 1.2. This highlights the very informative role of TAN network in
461 identifying the relationships amongst design variables towards the optimisation problem.
462 *4.2.1 Effect of each composition variable in lowering the global detrimental effect*
463 In order to better visualize the effect of each variable in lowering the global detrimental effect, represented
464 by the answer variable Y, the boxplots of the Y conditioned to each value of the design variables X_i,
465 i=1,…,4, is reported in Figure 12. Boxplots at the top-left present the distribution of Y values, when focusing
466 on a particular recycled aggregate. We can see that whilst NMcast as aggregate produces specimens with
467 value of Y ranging from 3 to 4, CMcast and NM have a wider range of Y values. Whilst the two different
468 values of water/binder ratio produce similar distributions of Y (boxplots at the top-right of Figure 12), it is
469 clear that using a percentage of air entraining equal to 0.09% produces in average low values of the response
470 (boxplots at the bottom-left of Figure 12). This behaviour can be explained by considering previous
471 researches that highlighted the effects of air-entraining agents, such as porosity increase, formation of larger
472 pores able to host large amount of salts prior to suffering detrimental effects, better interconnection of the
473 substrate with the porous structure of the render layer and enhanced moisture transport, [57-58].
474 Concerning the percentage of water repellent, whilst there are no statistically significant differences in the
475 distributions of Y when conditioning on 0.00% and 0.30% values, there is an increase of the median
476 response value when considering 0.50% of water repellent. The use of high percentages of water repellents

in presence of rising damp is known to have hindering effect of the liquid flux [38, 47]. This often leads to the recession of the evaporation front within the render layer, causing salt deposition within the layer and subsequently the sub-efflorescences formation and delamination. Despite this drawback when using the water repellent admixture, the experiment demonstrated that with low dosages, the internal salt solution flux is adequately regulated, whilst the protection against the entrance of external water is assured.

Focusing on the percentage of air entraining for which there is a clear difference in the response behaviour when conditioning on the two possible values, we notice that in Figure 13, when combined with a particular aggregate, the reduced percentage of the air entraining (0.03%) could provide a positive effect. For example, a specimen composed by the CMcast aggregate mixed at a 0.03% of air entraining, most of time leads to a response value Y in the optimality area of the experimentation, apart from one which has response Y=10 (ID experiment 2.3 of the second generation). To understand what could affect this experiment, we notice that this is the only mixture in which there is a percentage of water repellent equal to 0.5%, subsequently failure occurred due to preferential salt deposition within the first layer, delamination and detachment. A similar trend can be observed for NMcast, with higher value of Y with 0.03% of water repellent being associated with a 0.5% of water repellent in the external layer. When we consider mixtures added with NM, the use of 0.09% of air entraining agent is necessary to observe good durability, independently from the water-repellent's percentage of the external layer,the air entraining admixture possibly regulates the first layer's structure, allowing a good equilibrium of salt transport or storage during the cycles (as in 3.1).

5 Conclusions

The development of render systems able to endure in presence of salt solution and masonries contaminated by salts is still an open challenge for designers and manufacturers that often involves high research costs. The methodology applied in this study, effectively addressed the main goal of enhancing the durability of render systems exposed to the absorption/drying cycles of NaCl solution, by optimizing their compositions. Three generations were developed in order to obtain a significant reduction of the observed degradation forms, testing only 28 of experimental points out of 108 possible candidates.

The procedure, developed across three sequential generations, allows to prepare and test 7 systems at a time (28 specimens), that can be easily managed even in small and medium sized laboratories with low costs.

505 However, critical points were:

506 • the repetition of the procedure for each generation that requires long research times (1 month for the
507 specimens preparation and 1 month for the exposure and evaluation). Therefore, it is particularly
508 important to reach a significant optimization in few generations, as in our case;
509 • the definition of the response Y. We choose to define our target as a weighted sum of several decay
510 features. The weights were chosen on the basis of the severity of the decay forms, as commonly
511 considered in the conservation field (i.e. complete detachment over de-cohesion over external
512 crumbling over surface efflorescence);
513 • the evaluation of the degradation forms. The subjective nature of the "mark" influences the evolution
514 of the design process and the achieved results. In order to limit the subjectivity, the marks are given
515 by an expert researcher that integrates the impressions obtained by visual observation of the decay
516 extension and severity for each specimen with the results of quantitative measures of physical
517 behavior (weight and colour variations, flexibility, location of salts) .

518 The results highlighted that:

519 • the resistance to salt crystallization, tested by absorption and drying cycles of NaCl solution as
520 defined in [8], depends particularly on the correct use of water-repellent and air-entraining agents.
521 • Air-entraining dosage of 0.09% is suggested.
522 • Lower dosages of water-repellent (0% or 0.3%) reduce the degradation phenomena, possibly
523 allowing the solution flux till the surface and advection transport of salts.
524 • The recycled aggregate type did not show univocal trend and its effect must be considered in
525 association with the other variables. The use of cement-based aggregates containing water repellents
526 (CM750, CMcast) in association with 0,09% air entraining dosage diminished the render adhesion to
527 the brick and did not enhance the systems durability, whilst, the use of NHL-based aggregates (NM,
528 NM750, NMcast) with 0.09% air entraining content gave good results, most likely due to good
529 compatibility between aggregates and the NHL binder.

530 In order to better understand the renders effectiveness, the authors have envisaged further research
531 addressing the study of the transport mechanisms and salt depositions within the systems, based on the
532 investigation of the double layer microstructure, porosity and properties such as water absorption or drying

behavior. Moreover, future prospects foresee the application of the optimized system in meso scale models and on real historical masonries. The future testing should definitely confirm the renders suitability, however the results already obtained are promising for further application of this statistic methodology on a larger scale in order to optimize the render design reducing the research costs for the advantage of manufacturers and guarantying render effectiveness and compatibility for users satisfaction.

Acknowledgments

The Authors acknowledge Ca' Foscari Universtiy, DAIS department for funding the two-year grant "Physical degradation of historical masonries subjected to rising damp and remediation methods", the JPI EMERISDA Project "Effectiveness of Methods against Rising Damp in Buildings" and VICCS-UNIVE for funding a one-year grant "Impatto dei cambiamenti climatici sulle superfici architettoniche in ambiente Venezia" .
The authors want to thank Jade Straker for her linguistic support.

References

[1] B. Lubelli, R.P.J. Van Hees, C.J.W.P. Groot, Sodium chloride crystallization in a "salt transporting" restoration plaster, Cem.ConcreteRes. 36-8 (2006)1467–1474.
[2] B. Lubelli, R.P.I. Van Hees, H.P. Huinink, C.J.W.P. Groot, Irreversible dilation of NaCl contaminated lime–cement mortar due to crystallization cycles, Cem.ConcreteRes. 36-4 (2006) 678–687.
[3] B. Lubelli, M.R. de Rooij, NaCl crystallization in restoration plasters, Constr.Build.Mater 23 (2009) 1736–1742.
[4] T. Diaz Gonçalves, Salt crystallization in plastered or rendered walls, PhD thesis supervisor Delgado Rodrigues J, Universidade Técnica de Lisboa, Lisbon, 2007.
[5] G.W. Scherer , Stress from crystallization of salt in pores, in: 9th International Congress on Deterioration and Conservation of Stone, Venice, 2000.
[6] J. Petkovic´, H.P. Huinink, L. Pel, K. Kopinga, R.P.J. van Hees, Salt transport in plaster/substrate layers, Mater Struct 40 (2007) 475–490.
[7] J. Petkovic ´,H.P. Huinink, L .Pel, K. Kopinga, R.P.J. van Hees, Moisture and salt transport in three-layer plaster/substrate systems, Constr .Build. Mater. 24 (2010) 118–127.
[8] T. Wijffels, B. Lubelli, Development of a new accelerated salt crystallization test, in: Special Issue: COMPASS, Heron Journal 51-1 (2006), http://heronjournal.nl/51-1/2006_1.html
[9] Fragata, M. Rosário Veiga, A. Velosa, Substitution ventilated render systems for historic masonry: Salt crystallization tests evaluation, Constr. Build. Mater. 102- 1 (2016) 592-600.
[10] Groot, R. van Hees, T. Wijffels, Selection of plasters and renders for salt laden masonry substrates, Constr.Build.Mater 23-5 (2009) 1743–1750.
[11] M.A. Karoglou,A. Bakolas, N. Kouloumbi, A. Moropoulou, Reverse engineering methodology for studying historic buildings coatings: The case study of the Hellenic Parliament neoclassical building, Prog.Org.Coat. 72/ 1–2 (2011) 202-209.
[12] The Cement Sustainability Initiative (CSI), reports for http://www.wbcsdcement.org/ 2015 (accessed 12.12.2015).
[13] L. Barcelo, J. Kline, G. Walenta, E. Gartner, Cement and carbon emissions, Mater.Struct. 47 (2014) 1055–1065.
[14] Gulotta D., Goidanich S., Tedeschi C., Nijland T.G., Toniolo L., Commercial NHL-containing mortars for the preservation of historical architecture. Part 1: Compositional and mechanical characterisation, Construction and Building Materials 38 (2013) 31–42
[15] M. Stefanidou, E. Anastasiou, K. Georgiadis Filikas, Recycled sand in lime-based mortars, Waste Manage 34 (2014) 2595–2602.
[16] R. Raeis Samiei, B. Daniotti, R. Pelosato, G. Dotelli, Properties of cement–lime mortars vs. cement mortars containing recycled concrete aggregates, Constr.Build.Mater. 84 (2015) 84–94.
[17] JR Jiménez, J Ayuso, M López, JM Fernández, J De Brito Use of fine recycled aggregates from ceramic waste in masonry mortar manufacturing, , Construction and Building Materials 40 (2013) 679-690
[18] M Braga, J De Brito, R Veiga, Incorporation of fine concrete aggregates in mortars, Construction and Building Materials 36 (2012) 960-968
[19] P. Saiz Martínez, M. González Cortina, F. Fernández Martínez, A. Rodríguez Sánchez, Comparative study of three types of fine recycled aggregates from construction and demolition waste (cdw), and their use in masonry mortar fabrication, J.Clean.Prod. 118 (2016) 162-169.
[20] L. Senff, D. Hotza, W. L. Repette, V. M. Ferreira, J. A. Labrincha, Influence of added nanosilica and/or silica fume on fresh and hardened properties of mortars and cement pastes, Adv.Appl.Ceram.108-7 (2009) 418-428.

[21] R. Zaitri, M. Bederina, T. Bouziani, Z. Makhloufi, M. Hadjoudja, Development of high performances concrete based on the addition of grinded dune sand and limestone rock using the mixture design modelling approach, Constr. Build. Mater. 60 (2014) 8–16.
[22] Schackow, C. Effting, M. V. Folgueras, S. Güths, G. A. Mendes, Mechanical and thermal properties of lightweight concretes with vermiculite and EPS using air-entraining agent, Constr. Build. Mater. 57 (2014) 190–197.
[23] M.C.S. Ribeiroa, A. Fiúza, A.C.M. Castro, F.G. Silva, M.L. Dinis, J.P. Meixedo, M.R. Alvim, Mix design process of polyester polymer mortars modified with recycled GFRP waste materials, Compos.Struct. 105 (2013) 300–310.
[24] V. Ferrándiz-Mas,L.A.Sarabia,M.C.Ortiz, C.R. Cheeseman, E. García-Alcocel, Design of bespoke lightweight cement mortars containing waste expanded polystyrene by experimental statistical methods, Mater.Design 89 (2016) 901–912.
[25] R. Baragona, F. Battaglia, I. Poli Evolutionary statistical procedures, 2011, Springer-Verlag, Berlin.
[26] D. Slanzi, I. Poli, Evolutionary Bayesian network design for high dimensional experiments, Chemometr. Intell. Lab. 135 (2014) 172–182.
[27] D. Slanzi, D. De Lucrezia, I. Poli, Querying Bayesian Networks to design experiments with application to 1AGY serine esterase protein engineering, Chemometr. Intell. Lab. 149, Part A (2015) 28-38.
[28] M. Borrotti, D. De March, D. Slanzi, I. Poli, Designing lead optimisation of mmp-12 inhibitors, Comput. Math. Method. M., vol 2014(2014)1-8.
[29] J. Pearl, Probabilistic Reasoning in Intelligent Systems: Networks of Plausible Inference. Morgan Kaufmann, 1998.
[30] R.G. Cowell, A.P. Dawid, S.L. Lauritzen, D.J. Spiegelhalter, Probabilistic Networks and Expert Systems. Springer-Verlag, 1999.
[31] D. Koller, N. Friedman, Probabilistic graphical models: principles and techniques — adaptive computation and machine learning, The MIT Press, 2009.
[32] K. Korb, A. Nicholson, Bayesian Artificial Intelligence. Chapman & Hall/CRC, 2010.
[33] M. Scutari, J. Denis, Bayesian networks: with examples in R, Chapman & Hall/CRC Texts in Statistical Science, Taylor & Francis, 2014.
[34] M. Forlin; D. Slanzi; I. Poli, Combining Probabilistic Dependency Models and Particle Swarm Optimization for Parameter Inference in Stochastic Biological Systems. In: FL Gaol, QV Nguyen (Eds), Proceedings of the 2011 2nd International Congress on Computer Applications and Computational Science, Springer, vol. 145 (2012) 437-443.
[35] M. Borrotti, I. Poli, Nave bayes ant colony optimization for experimental design. In: R. Kruse, M.R. Berthold, C. Moewes, M.n. Gil, P. Grzegorzewski, O. Hryniewicz (Eds.), Synergies of Soft Computing and Statistics for Intelligent Data Analysis, Vol. 190 of Advances in Intelligent Systems and Computing, Springer, Berlin Heidelberg (2013) 489–497.
[36] J. Lanas, P. Bernal, M.A. Bello, A. Galindo, Mechanical properties of natural hydraulic lime-based mortars. Cem Concrete Res. 34-12 (2004) 2191-2201.
[37] B.A. Silva, A.P. Ferreira Pinto, A. Gomes, Natural hydraulic lime versus cement for blended lime mortars for restoration works, Constr.. Build.Mater. 94 (2015) 346–360.
[38] L. Falchi, U. Müller, P. Fontana, F.C. Izzo, E. Zendri, Influence and effectiveness of water-repellent admixtures on pozzolana–lime mortars for restoration application, Constr. Build. Mater. 49 (2013) 272–280.
[39] M. Lanzón, P.A. Garcia Ruiz, Effectiveness and durability evaluation of rendering mortars made with metallic soaps and powdered silicone, Constr Build Mater 22 (2008) 2308-2315.
[40] L Falchi, C Varin, G Toscano, E Zendri, Statistical analysis of the physical properties and durability of water-repellent mortars made with limestone cement, natural hydraulic lime and pozzolana-lime. Constr. Build.Mater. 78(2015) 260–270.
[41] P.L. Gaspar, J. de Brito, Quantifying environmental effects on cement-rendered facades: A comparison between different degradation indicators, Build.Environ. 43 (2008) 1818–1828.
[42] J. Delgado Rodrigues, A. Grossi, Indicators and ratings for the compatibility assessment of conservation actions, J.Cult.Herit. 8 (2007) 32-43.
[43] J.Grilo, A Santos Silva., P.Faria, A.Gameiro, R. Veiga, A. Velosa, Mechanical and mineralogical properties of natural hydraulic lime-metakaolin mortars in different curing conditions, Construction and Building Materials 51 (2014) 287–294
[44] S. Barr, W.J. Mc Carter,B. Suryanto, Bond strenght performance of hydraulic lime and natural cement mortared sandstone masonry, Construction and Building materials 84 (2015) 128-135
[45] M.P. Seabra, J.A. Labrincha, V.M. Ferreira, Rheological behaviour of hydraulic lime-based mortars, Journal of the European Ceramic Society 27 (2007) 1735–1741
[46] G. Cultrone, E. Sebastia ´n, M. Ortega Huertas, Forced and natural carbonation of lime-based mortars with and without additives: Mineralogical and textural changes, Cement and Concrete Research 35 (2005) 2278 – 2289
[47] T. Zhao, F.H. Wittman, R. Jiang, W. Li, Application of silane-based compounds for the production of integral water repellent concrete, in: E.Borelli, V.Fassina (Eds.), Proceedings of Hydrophobe VI, 6th international conference on water repellent treatment of building materials, Aedificatio Publisher, Freiburg, 2011, pp 137-144.

[48] L. Falchi,E. Zendri, E. Capovilla, P. Romagnoni, M. De Bei., The behaviour of water-repellent mortars with regards to salt crystallization: from mortar specimens to masonry/render systems, Mater Struct (2017) 50: 66.
[49] UNI8941:1987 coloured surface- colorimetry, principles, colour measurement, calculation of colour differences
[50] Schmidt OS-120PT, information illustrating the device and its use available at: https://www.proceq.com/compare/schmidt-rebound-hammers/; https://www.proceq.com/uploads/tx_proceqproductcms/import_data/files/Schmidt%20OS-120_Operating%20Instructions_English_high.pdf; https://youtu.be/wZOuJ7L5ojI; (last access 14/03/2017)
[51] Normal 13/83 Dosaggio dei Sali solubili totali mediante misure di conducibilità (italian normative on stone material- determination of the content of soluble salts with conductivity measurments) 1983.
[52] J.B.O Mitchell, Machine learning methods in chemoinformatics. Wiley Interdisciplinary Reviews: Computational Molecular Science, 4-5(2014) 468-481.
[53] M. Ramoni, P. Sebastiani, Robust Bayes classifiers, Artiff. Intell., 125-1 (2001) 209–226.
[54] N. Friedman, D. Geiger, M. Goldszmidt, Bayesian Network Classifiers, Mach. Learn., 29-2/3 (1997) 131-163.
[55] C. Bielza, P. Larrañaga, Discrete bayesian network classifiers: A survey. ACM Comput. Surv., 47-1 (2014), nr 5.
[56] The R Project for Statistical Computing. www.r-project.org
[57] H.F.W. Taylor, Cement Chemistry, Second ed., Academic press, London, 1997.
[58] H.N. Atahan, C. Carlos Jr., S. Chae, P.J.M. Monteiro, J. Bastacky, The morphology of entrained air voids in hardened cement paste generated with different anionic surfactants, Cement Concrete Comp. 30-7 (2008) 566-575.

Optimization of sustainable, NaCl-resistant and water-repellent renders through evolutionary experimental design

Laura Falchi[a*], Debora Slanzi[a, b], Laura Speri, Irene Poli [a, b], Elisabetta Zendri[a]

[a]Department of Environmental Sciences, Informatics and Statistics, Ca' Foscari University of Venice; Via Torino 155 eta, 30170, Mestre (Venice), Italy; Phone +39 041 2346732; laura.falchi@stud.unive.it; elizen@unive.it;

[b]ECLT, European Centre for Living Technology, Ca' Minich, S. Marco 2940 30124 Venezia, Italy; debora.slanzi@unive.it; irenpoli@unive.it

***Corresponding Author.**
Laura Falchi

Department of Environmental Sciences, Informatics and Statistics, Ca' Foscari University of Venice; Via Torino 155 eta, 30170, Mestre (Venice); Italy

Phone +39 041 2346732

laura.falchi@stud.unive.it

Abstract

The paper deals with the formulation of salt-resistant renders, suitable for the protection of brick masonries subjected to rising damp of salt solution. Natural hydraulic lime, recycled mortars as aggregates, air entraining and/or water-repellent admixtures were selected to produce a double layer render ~~system to guarantee eco- and historical-compatibility and~~ resistan~~ce~~t to the action of NaCl solution ~~salts~~. The render formulations were optimized by an evolutionary experimental design approach based on Bayesian networks, namely EBN-design, in order to minimize physical damages such as detachments, scaling, efflorescences. Results show that this innovative approach is promising for discovering NaCl-resistant renders by experimentally testing just a limited number out of the possible compositions.

Comment [LF1]: Abstract - There's still too much emphasis on eco and historic compatibility given that: (i) the real topic of the article is the resistance to salt crystallization; (ii) these two features are not accessed in the article and, so there is no real guarantee that they are met. As I see it, this kind of generalization lowers, rather than increases, the credibility of the article. I would suggest rewriting the second sentence to something like: "… to produce a double layer system resistant to salt crystallization, which is also as much as possible eco-sustainable and compatible with old masonry".

Keywords: Render; Salt Resistance; Recycled Wastes; Evolutionary Design of Experiment; Bayesian Networks; Natural Hydraulic Lime; Water-Repellent admixtures; Air-entraining agents

1. Introduction

1.1 Repairing renders for historical masonries affected by rising damp of marine water

Severe decay of render systems occurs in marine environments due to salty water penetration, salt deposition, sub-efflorescences formation, salt efflorescences, and physical shrinkage occurring at each crystallization/dissolution cycle [1-8]. Render systems, appropriately calibrated, have demonstrated to tackle the problem by regulating the water flux and salt transport [6-10]. The technical literature describes several renders types developed, studied and applied for the protection and conservation of architectural and historical masonries, among them: traditional renders with slight hydraulic properties or cement composites with high hydraulic properties; slow transporting and water-proof layers or macroporous, highly permeable and sacrificial plasters [6-8].

However, the development of render mixtures durable in marine environments and suitable for historical masonries restoration remains a complex challenge. Several issues have to be taken into account: i) the system effectiveness, in terms of resistance to the disaggregating action of salts, internal cohesion, adhesion to the substrate, external appearance, etc. [9]; ii) the compatibility of the render systems with the historical masonry in chemical-physical terms, as stated in [10-11], iii) the increased awareness regarding eco-sustainability that leads to prefer environmental compatible systems [12-13]. Compatibility and eco-sustainability can be addressed by choosing natural hydraulic lime NHL instead of cement as binder (NHL in fact repeatedly demonstrated a general compatibility with ancient masonries and lower carbon footprint [[12; 14]) and recycled materials as aggregates [15-19]. Effectiveness can be addressed by opportunely testing laboratory specimens, subsequently individuating the most promising systems, optimizing the starting composition to on-field apply and test.

In this study, an evolutionary experimental design approach is presented for the i) evaluation of renders durability when exposed to 3% NaCl solution and the ii) in-lab optimization of render system formulation.

1.2 Optimization of the mixture formulation by experiment design methods

In the traditional approach, owing to his/her expertise, the researcher individuates the suitable starting materials, mix proportions, application and curing conditions, then he/she tests some promising compositions. Since testing all the possible compositions is not economically sustainable, only few compositions are selected: the choice is strictly related to the researcher's experience and previous well-

known literature. However, the expert's subjective knowledge on mixture compositions can prevent to select and test promising compositions *a priori* excluded from the experimentation

In the last few years, studies based on statistical designs of the experiments (DoE) and on mixture design modeling are becoming more widespread and offer an alternative approach to the optimization of render formulation.

Through factorial experimental designs, the effects and possible interactions of the different material factors can be assessed (chemical admixtures, mineral additions and water/binder ratio). In k^d factorial designs, a set of possible compositions is defined, where d represent the number of factors (e.g. binders, aggregates, admixtures) and k represents the number of possible levels for each factor (e.g. tot. binder types, tot. different aggregates, tot. different water-repellent percentages) . Analysis of the variance (ANOVA) is then developed on the results of suitable physical properties (e.g. the maximum compressive strength or the capillary water absorption coefficient) to test if any factor produces a statistically different effect on the responses [20-22]. For example, Ribeora et al (2013) [23] evaluated the effect of selected factors such as expanded polystyrene addition content and type ~~, cement type~~ and a superplasticizer-water-retaining mix with ANOVA built on a 2^1x4^1 mixed-level full factorial design on capillary absorption and compressive strength, whereas Ferrandiz et al (2016) [24] proposed a 3^3x2^1 d-optimal experimental design to evaluate the effect of incorporation of recycled glass fibre reinforced plastics on the mechanical behaviour of polyester polymer mortars. These DoE approaches generally requires to experimentally test almost all or even all the possible combinations; therefore they are suitable when a very limited number of factors and/or levels of factors are investigated. Moreover, to develop analysis on the effect of the factors or interactions amongst factors, simple models with a small set of interactions are usually assumed.

Comment [LF2]: Lines 73-75 "For example, Ribeora et al (2013) [23] evaluated the effect of selected factors such as expanded polystyrene addition content and type, cement type and a superplasticizer-water-retaining mix with ANOVA built on a 2^1x4^1 mixed-level full factorial design on capillary absorption and compressive strength…" - I think there's something wrong here. 2^1x4^1 => we have 1 factor with 2 levels and 1 factor with 4 levels, that is, a total of 2 factors. However, 3 factors are mentioned before (expanded polystyrene, cement and superplasticizer).

While the number of variables and their different nature, as well as the limited number of points that can be tested due to technical and economical constraints, can make it very difficult to use classical DoE methodologies, planning efficient and effective experiments is essential to achieve good results in such areas of research where experimentation is complex, extremely expensive and time consuming.

In this study, an innovative approach based on evolutionary experimental designs is proposed: the Design of Evolutionary Experiments based on Models approach (DEEM approach) [25-28]. DEEM approach has been recently developed to derive small sets of informative experimental points (i.e. to experimentally test a

limited number of compositions), when classical hypotheses of statistical designs and multidimensional modelling are missing.

The design, consisting of a collection of experimental points, is regarded as a population that evolves across generations according to the evolutionary paradigm. Each population of experiments is very small with respect to the size of the possible designs (i.e. all the possible combinations according to the variables and their levels), but it changes throughout generations, "learning" from one generation to the next and exploring, in an intelligent way, the search space.

Statistical models are used to identify the relevant information at each generation and this information is incorporated in the evolutionary procedure, making the search more efficient and effective. In particular, our approach is based on the evolution of Probabilistic Graphical Models, PGMs [29-31], i.e. models where a graph-based representation is combined with the rules of probability theory to provide a flexible framework for modeling large collections of variables with complex interactions. We focus on a particular class of PGMs, that is the class of Bayesian network models (BNs), where the graph representation is based on nodes corresponding to random variables and on arcs between nodes, describing the probabilistic dependence structure that may characterize the set of variables on which we then develop statistical inference [32-33].

When a limited number of experimental points, i.e. promising compositions, can be tested due to technical and economical constraints, the information achieved by statistical models is adopted to guide the optimization towards the objective of the experiment. The "optimal composition" can be defined in relation to specific environmental situations and to desirable properties, allowing a good durability and compatibility.

DEEM approach is very flexible, since it can be developed using different classes of models and with different evolutionary procedures. Moreover it has the great advantage of significantly limiting the experimental tests (in our case just 30% of the possible combinations were experimentally tested) and it has been proved to produce very successful results in a large set of experimental studies [26-28; 34-35].

1.3 Aims and structure of the work

In this study, the specific aims were:

- to individuate render multilayer systems able to resist to rising damp of 3% NaCl solution and to minimize the degradation patterns such as detachments, disaggregation, sub- and efflorescence formation;
- the individuation of the promising systems within a large and complex set of possible compositions by applying DEEM approach based on Evolutionary Bayesian Network models, in order to avoid *a priori* and subjective decision of few testable mixtures;
- to highlights strengths and weaknesses of this approach when applied to the development of complex render systems.

Double layer render systems on bricks specimens, based on natural hydraulic lime NHLas binder and recycled crushed mortars were considered. Moreover, air-entraining agents, water repellent admixtures, different water binder ratios, were taken into account in order to act on porosity and wettability which are usually related to the salt- resistance, as highlighted in previous researches [2-7, 36-40]

The systems, produced according to the indication of the experimental design, underwent cycles of capillary absorption of 3% NaCl solution and drying cycles to simulate the effect of marine water.

Subsequently, visual observation, weight variations, the capability to remain adherent to the brick under mechanical solicitation and salt distribution were assessed. Based on the results and on an expert elicitation [41-42] four detrimental effects, i.e. the presence of detachments, internal de-cohesion and crumbling, external erosion/exfoliation and external efflorescences, were identified as response variables Y_i and evaluated with a mark. This mark, chosen in a 10-point scale ranging from 1 to 10, was assigned to each detrimental effect and considered as observed value of the associated response variable. ~~Then a model among response variables and design variables were estimated to infer the next generations of experiments~~. Then a statistical model built for both response variable and design variables were estimated from the available data. The successive generation of experiments was therefore determined by predicting the estimated behaviour of the system variables by means of the information achieved from the statistical model.

The process was repeated three times in order to minimize the degradation effects and optimize the system behaviour.

Comment [LF3]: Then a model among response variables and design variables were estimated to infer the next generations of experiments." - I don't understand this sentence

Following the evolutionary characteristic of the proposed approach, in this paper we present the results obtained for each tested generation, and finally the model achieved at the end of the process is presented and discussed.

2. Materials and Methods

2.1 Starting Materials and design variables

Table 1 summarizes the brick substrate, the double layer render system and its general composition.

In order to resemble a traditional masonry, full, red-fired bricks (by San Marco Laterizi S.p.A., dimensions 16cm X 12cm X 2cm) were chosen as substrate for the render application.

The preparation of the first layer of render involved the following starting materials: natural hydraulic lime NHL 3.5 supplied by MGN as binder; limestone- siliceous sand with a size fraction of 0/5 mm as aggregate; recycled aggregates (size fraction 0/5, Boloomey distribution, obtained by crushing old water-repellent mortars made of limestone cement, natural hydraulic lime and pozzolana-lime [38; 40]); sodium alkyl sulfonate admixture as air entraining agent; tap water used in two different water–binder proportions.

For the preparation of the second layer NHL 3.5, a limestone- siliceous sand (size fraction 0/2 mm) and water repellent admixtures (calcium stearate by SIGMA Aldrich or the powdery siloxane product Sitren P750 by Evonik) were employed.

.In order to design optimal renders with respect to specific properties, we defined the set of design variables $\mathbf{X}=(X_1,X_2,X_3,X_4)$, where each X_i represents a particular component of the specimen (Table 1):

- X_1: Recycled aggregate, assuming the set of possible values x_1={CM, CM750,CMcast, PM, PM750, PMcast, NM, NM750, NMcast}
- X_2: water/binder ration, assuming the set of possible values x_2={1.0, 1.2}. These levels were chosen in order to obtain to obtain either a regular mixture workability, either a fluid mixture with a final higher porosity [43-44]
- X_3: % of air entraining, assuming the set of possible values x_3={0.03, 0.09}. The three possible ratios were chosen for the air entraining agents in order to obtain different microstructures and porosity, in particular the second ratio is a percentage commonly used in dry-mix products, whilst the third is able to obtain a macroporous structure [45-46]

- X_4: % of water repellant, assuming the set of possible values x_4={0, 0.03, 0.05}. These ratios are commonly used in commercial products and in previous researches [36, 38, 47].

Under this setting the whole combinatorial search space Ω consists of 9*2*2*3=108 possible specimens types (experimental points). Applying DEEM approach based on Evolutionary Bayesian Network, EBN-design, we limit the number of candidate experimental points to 28 representing just the 26% of the tests to be conducted. Since each experimental point corresponds to three replicated specimens, 84 specimens were physically produced out of 324 theoretical specimens.

2.2 Specimens preparation and exposure

The composition of each specimen was indicated by EBN-design in each generation of the procedure (see also paragraph 2.4), whilst their preparation and exposure is based on the Protocol proposed within the COMPASS project [8]. The choice of the testing protocol is particularly difficult when the resistance to salt degradation of multicomposite systems is considered, since no precise normative is available [48], the COMPASS protocol was chosen since it demonstrated to be particularly suitable in highlighting salt-induced degradation. Mock-ups made of full, fired clay bricks, covered by a double layer of render were prepared (Figure 1). The preparation of the first layer involved mixing of the binder with half the water and with the air entraining agent at a low speed (100 rpm) for 5 minutes, then the remaining water and the aggregates were incorporated and mixed for a further 5 minutes. The mixture was then applied on moist bricks to form a layer 1 cm thick and patting the surface with a trowel in order to enhance the adhesion of the second layer. The specimens were cured for 12 hours at 95% HR and 20°C before the application of the second layer. The second layer, 0.5 cm thick, was prepared by applying the mixture of binder, water, aggregates and water repellent admixtures (when present) on the first layer, then smoothing the surface with a trowel. The specimens were cured in environmental atmosphere at 95% HR and 20°C for 28 days, then dried at room temperature till constant weight (HR% 55%, T 23 °C). Three independent replicates were prepared for each experimental point. The major differences with the COMPASS protocol are the larger dimension of the specimens (16cm x12cm x2cm) and the absence of lateral sealing, in order to enhance mocks-up representativeness.

Once hardened, each system was subjected to drying-wetting cycles by capillary rise of 3% by weight NaCl solution, in order to simulate the salinity of the sea water. The bottoms of the specimens were immersed in the salt solution for 24 hours to ensure complete wetness also in the presence of water repellent admixtures. The specimens were then removed from the container and placed at HR 65%, T23°C for a 7 day drying, thus avoiding excessive stress on the material and allowing the evaporation of 80% of the solution before the following cycle. Four cycles were performed in one month of exposure without removing efflorescence or debris from the surface of the specimens at each cycle.

2.3 Evaluation methods

In order to highlight the resistance to salt crystallization cycles, the specimens were weighted at each cycle, while photographic documentation and 1200dpi scans of the surfaces by a Epson perfection 3170 Photo was taken after the cycles to record the presence of decay forms such as efflorescences, cracks, erosions linked to the extension of stains, crusts and eroded areas. The visual damage was revealed also by optical microscopy observations with a DINO-lite Premier AM4113T microscopy (10-200x), 1.3 MPx. Moreover, colorimetric measurements were performed using a CM2600d Konica Minolta portable spectrophotometer with aD65 illuminant and 10° standard observer to quantify the SCI (Specular component included) colour variations due to erosion or salt crusts formation [49]. In order to consider the high surface inhomogeneities and obtain a repeatable measure, a medium averaged spot size of 8 mm Ø, an average of 5 points with 3 scans each was considered for each specimen. The formation of salts crusts and efflorescences on the surfaces lead to more or less extended white stains with lightness increase over 5 points, the formation of sub-efflorescences lead to delamination and erosion of the surfaces with lightness decrease over 5 points.

In order to evaluate the internal degradation and possible detachment of the render layers enhanced by salt crystallization, a Schmidt Pendulum Hammer PT sclerometer for soft materials was used. The instrument measures the rebound of a spring loaded mass impacting against the surface of the sample., The mass is constituted of a cylindrical hammer head of 40mm diameter and 720g that slides on an arch, the hammer head can be loaded in fixed position, then released in order to impact the surface with an impact energy of 0,83Nm or 0,44J [50] . The strokes give a reproducible mechanical solicitation that might cause detachment

Comment [LF4]:
The authors used "an analogue instrument composed by a pendulum" to observe the rebound angle. The authors should insert a figure of the pendulum hammer device to illustrate this device.
Video uso sclerometro anche Schmidt
https://youtu.be/wZOuJ7L5ojI

in inlgese:
https://www.proceq.com/compare/schmidt-rebound-hammers/

http://www.pasisrl.it/ftp/prd/pdf/Schmidt_Family_Sales_Flyer_IT_2013.04_high.pdf

or failure of degraded layers and the rebound is dependent to the hardness of the material (tabulated in specific graphs by the instrument producer). Five hammer strokes at percussion energy 0.44J were followed by other five at 0.8~~8~~3J, by choosing a different starting angle of the pendulum. The specimens that endure all the strokes without failures or detachments demonstrated optimal cohesion and salt resistance, moreover, the higher the rebound, the stronger the internal render cohesion.

The salt distribution profile at the end of the test was used as an indication of salt transport within the plasters and the possibility to sub-surface damage. The renders were cut without the use of water in 4slices, and the conductivity was determined according to NorMaL 13/83 with the EC-meter GLP31 by Crison [~~50~~51].

To evaluate the quality of each candidate point, i.e. the overall resistance of each system to salt decay, four parameters of decay (i.e. response variable Y_i, i=1,..,4) were selected and evaluated by using the results of the observations and measurements and by elicitation of the researcher. In order to guarantee an opportune of elicitation, the researcher should have sufficient background experience to autonomously identify the typical degradation patterns, the properties and behaviour of render systems suitable for historic masonries. The parameters, selected for their severity and representativeness, are:

- Y_1=presence of detachments and cracks formation (the behavior after the mechanical solicitation with Schimdt Hammer is considered, together with visual observation of cracks);
- Y_2=internal de-cohesion and crumbling (hardness and elastic properties measured by the hammer rebound is considered together with mass losses and visual observation);
- Y_3=external erosion/exfoliation (visual observation, erosion extent, colorimetric measurements and position of salts by conductivity measurement are taken into account);
- Y_4=external efflorescences (white stains and crusts extent and colour variation are considered).

Each response variable is evaluated with a mark from 1 to 10, where 1= non present; 10= completely present, e.g. Y_1= 10 if complete detachment of the render layer from the substrate occurs without hammer strokes or with low energy strokes (0,44J), Y_1=1 if no detachment occur after 10 strokes; Y_2=8-10 if negative mass losses ($\Delta M\% \leq -2$) and low rebounds (≤ 8) are measured; $Y_{3,4}$= 10 if the degradation extent cover the whole

Comment [LF5]: The authors based their model on visual assessments and on expert knowledge, saying that "the expert guarantees an objective evaluation that takes into account several things and not a mere transformation of physical data into marks". The authors should discuss better the skills of this "expert" and the scientific and/or professional background that allow an accurate assessment.

surfaces, $Y_{3,4}$ =1 if it covers less than 20% of the surface. The averaged results of the three replicates for each experimental point is considered.

We can then assume that these decay forms have decreasing importance; in fact the render and the masonry undergo severe damage if the render is completely detached or if its internal cohesion is scarce due to salt action; external exfoliation and erosion cause surface damage limited to the render; external efflorescences do not physically damage the masonry or render, but might induce prolonged render wetness due to salt hygroscopicity and aestethical damage. Therefore, in order to define a unique response function Y to optimize, we will introduce a weighted combination of the selected parameters defined as

$Y=0.4Y_1+0.3Y_2+0.2Y_3+0.1Y_4$.

2.*4 DEEM approach based on Evolutionary Bayesian Networks (EBN-design)*

The DEEM approach based on Evolutionary Bayesian Networks, EBN-design, begins by randomly generating a first population of n_1 experimental points $\mathbf{X}_{n1}=(\mathbf{x}_1\ \mathbf{x}_2\ldots\mathbf{x}_{n1})$, where each point $\mathbf{x}_k=(x_{k,1}x_{k,2}x_{3,k}x_{k,4})\in\Omega$, k=1,…, n_1, represents the particular combination of components producing a specific specimen.

This initial design is then prepared and tested as described in paragraph 2.2. The degradation patterns were evaluated as described in Paragraph 2.3 thus providing the first set of response values, namely the vector y_{n1}. At the end of this step the set of data $D_1=(\mathbf{X}_{n1},\ \mathbf{y}_{n1})$ representing both the tested specimens and their corresponding observed responses, is available for the first generation.

This set of data is modeled by a Bayesian network models, which is formally represented by a directed acyclic graph (DAG) and a probability distribution (P). DAG represents the structure of the BN and it is composed of nodes representing the set of random variables $X=(X_1,X_2,...,X_d)$, each of which can take a value in a finite set of possible mutually exclusive variable values, and of arcs between nodes in the form of $X_i\rightarrow X_j$, indicating direct probabilistic dependencies between the corresponding variables. The correspondence between the structure of the DAG and the dependence and independence relationships among the variables is derived by the d-separation criterion [31-32]. This criterion in fact uses the properties of the path structures and graph theory to define whether two nodes are independent conditioned to another node or set of nodes. Then from the identification of the dependence/independence relationships, the Markov

property is assumed stating that there are no direct dependencies in the system being modeled which are not already explicitly shown via arcs and d-separation [31-32]. Finally by means of the Markov property, the joint probability distribution P can be written as in the following factorization:

$$P(\mathrm{X}=\mathrm{x})=\prod_{i=1}^{n} P(X_i=x_i|Pa(x_i)) \qquad \mathrm{i}=1,\ldots,\mathrm{d} \quad (1)$$

where $\mathbf{X}=\mathbf{x}$ indicates that the set of variables $\mathbf{X}=(X_1,X_2,...X_d)$ is observed at specific values $\mathbf{x}=(x_1, x_2, \ldots x_d)$, and $Pa(x_i)$ is regarded as the particular value realization of the parent set of X_i, i.e. all the variables with a direct arc to X_i. The set of conditional probabilities $P(X_i=x_i|Pa(x_i))$, i=1,...,d, represents the set of parameters of the Bayesian network. The simplification of the joint probability distribution given by Eq.1 allows complex systems to be analyzed and modeled using a limited number of local relationships and to be regarded as stochastic models, built up by combining together simple components.

When a particular target variable Y, i.e. class variable, is identified within the set of variables, we can see the Bayesian network as a probabilistic classifier [32, 521]. These classifiers are used in many applications as they are able to probabilistically identify to which target value a new observation belongs based on the observation of the values assumed by the other variables of the system. In particular, Bayesian classifiers such as Naive Bayes [532] or Tree Augmented Naive Bayes, TAN [534-545] are graphical models composed of nodes and arcs among nodes with particular structures. Naïve Bayes assumes that the target variable Y has a direct dependence relationship with all the X_i variable of the system, $Y \rightarrow X_i$, but no dependencies are admitted among the set of X_i; TAN relaxes this assumption assuming that the target variable Y has no parents and each variable X_i has as parents the target variable and at most one other variable X_j. In this research we will focus on TAN classifiers as they are a restricted family of Bayesian networks and they are proven to perform very well in chemoinformatics applications [512].

Following EBN-design we built a TAN classifier and used the achieved joint probability distribution to predict the estimated values $\hat{y}_{1,\Omega}$ of the class variable for all the possible points of the search space. From the set of values $(\Omega,\hat{y}_{1,\Omega})$ we select the sub-set of n_2 experimental points with optimal predicted class values. This new set of points $\mathbf{X}_{n2}=(\mathbf{x}_1\,\mathbf{x}_2\ldots\mathbf{x}_{n2})$ becomes the second population of the evolutionary procedure and is evaluated yielding the new data $D_2=(\mathbf{X}_{n2}, \mathbf{y}_{n2})$.

This process is iteratively repeated, generation after generation, and ends when total number of experimental

Formatted: Not Highlight

points is tested. In particular in this experimentation we build EBN-design selecting a population of n_q=7 specimens and evolving the algorithm through 3 generations, i.e. q=1,2,3. Only for the first generation, as we need to test all the recycled aggregates (the 9 possible values of variable X_1), we randomly select 14 candidate experimental points by assuming that all the aggregates were selected almost once. With this design setting, we then evaluate only 28 possible candidate specimens representing 26% of the whole search space. EBN-design and all the statistical analysis were performed using the R statistical software [~~55~~56]

3. Results

Table 2 reports the mixture compositions of the specimen population defined in the three generations. The three generations were prepared and tested separately and subsequently, since the results of each generation was used to estimate a model of the experimental space and to indicate the optimized mixtures for the next generation. Therefore, the discussion is presented by highlighting the results of each sequential generation.

3.1 First generation

After 28 days of maturing, some of the render layers detached bodily from the bricks, even before the crystallization cycles, as indicated in table 3 and shown in Figure 2. Y_1 (detachments) was evaluated as 10 when bodily detachment occurs before the exposure.

Besides the detached specimens, the more recurrent decay features were (Figure 2): slight presence of efflorescences without substantial loss of material and slight darkening of the surface for the series 1.7 and 1.1; diffuse presence of efflorescence (1.2,1.3, 1.4, 1.11); spalling and surface delamination (1.13, 1.14,1.5); diffuse delamination and complete detachment from the surface layer (1.6, 1.8, 1.9, 1.10). The variations of colour components a* and b* are negligible, whilst ΔL^* and the total variation ΔE are almost coincident. The prevailing colour of the mortars is gray and the salts can cause white efflorescences or a darkening effect (hue saturation) due to surface erosion or hygroscopic humidity retention(Figure 3).. The series 1.5,1.4,1.2, 1.10 were affected by a higher absolute colour variation, with darkening mainly due to loss of the external layer in the case of 1.5, 1.10 and to hygroscopic humidity for 1.4 and 1.2.

334 The weight variations seem to reflect the appearance of the specimens (Figure 4): weight variation of series
335 1.1 to 1.6 is not significant and a lesser presence of salt crusts and efflorescences were observed, while
336 positive weight variation were observed for the series 1.10, 1.11, 1.13, 1.14 due to salt accumulation within
337 and over the specimens, evident also by visual observation. The differences at each cycle could be due to a
338 different drying behavior of specimens more polluted by salts.
339 Before the exposure, the different series showed similar conductivity of around 42±10 μs/cm in the internal
340 layer and 70±20 μs/cm in the external layer. After the exposure, the conductivity profiles (Table 3) indicate
341 that most of the specimens accumulate salts close to the surface, pointing out the presence of efflorescences
342 or subefflorescences. In particular, the series 1.1, 1.3 maintained high salt concentration in the whole profile;
343 1.7 and 1.11 (with 0.5% and 0.3% of water repellent on the external layer) shown salt accumulation behind
344 the surface; 1.2 maintained a uniform increasing profile; 1.8 (without water repellent admixture) showed a
345 lower conductivity in the middle layers.
346 Hammer rebound test (table 3) highlighted that series 1.3, 1.6, 1.14, 1.10, did not detach before the salt
347 cycles and were able to endure 7 strokes before bodily detachment, even if the mean hammer rebounds
348 values were around 10, denoting soft mortar layers. 1.9 and 1.13 also demonstrated an acceptable adhesion
349 before the cycle (1 specimen over 3 detached by themselves) and after the cycles, by enduring at least 9
350 strokes. In every case, high standard deviation were calculated, due to the intrinsic heterogeneity of the
351 systems, which caused rebound variation within each specimen.
352 Based on the observed behaviour, in particular on the absence/presence and extent of the different
353 degradation pattern Y_i, the marks assigned to the specimens of Generation 1 are reported in Table 4 (rows 1-
354 14).
355
356 ***3.2 Second generation.***
357 Table 2, rows 15-21, reports the mixture compositions (2.1-2.7) of the population provided for the second
358 generation from the information achieved by TAN model estimated for the response variable Y, i.e. the mark
359 of the specimens, and design variables, i.e. specimen components.
360 After 28 days of curing and the first drying, the render layers of set 2.3, 2.4, 2.5 detached bodily from the
361 bricks, pointing out a lack of flexibility and an insufficient adhesion (Table 3).

362 The exposure caused recurring patterns within each set of specimens (Figure 2), in particular: 2.2 was the
363 unique set showing scarce crumbling and few salt efflorescences on the surfaces, whilst 2.4 and 2.5
364 specimens were covered by salt efflorescences, serious erosion of entire surface areas occurred. The
365 colorimetric measurements shown in Figure 5 agree with the visual observation, denoting a lightness ΔL*
366 and total colour ΔE variations were higher than the first generation, in particular for 2.4 and 2.2.
367 The salt accumulation within and over the specimens caused a common increasing trend regarding weight
368 variation during the cycles (Figure 6). Weight discrepancies were observed particularly after the first cycle,
369 possibly due to a higher salt transport and accumulation, without crumbling or material losses, in comparison
370 to the following cycles. Then, spalling and crumbling occurred with loss of material, counterbalancing the
371 salt accumulation and efflorescence formation. The relative variation amongst the different sets could be due
372 to different presence of salts in relation to the water repellent behavior, the pore structure and the
373 hygroscopicity of the systems.
374 Also for the second generation, the conductivity measurements indicate (table 3) a higher salt concentration
375 in the external parts of the systems in comparison to internal parts, due to deposition of salt on the surfaces.
376 However, 2.1, 2.2 and 2.6 had high concentration also nearby the brick.
377 In comparison to the first generation, the different series endured higher mechanical solicitation with at least
378 9 strikes before bodily detachment. In particular, 2.4 and 2.6 demonstrated optimal adhesion even after
379 repeated strikes and rebounds over 20°, denoting a coherent, but still elastic structure.
380 Marks assigned to the specimens of Generation 2 are reported in Table 4 (rows 15-21).
381
382 ***3.3 Third generation***
383 The mixture compositions defined in the third generation, achieved by modeling marks of the first and
384 second generation, are presented in table 2, rows 22-28.
385 In this generation just one specimen underwent bodily detachment from the brick before the exposure. After
386 the cycles, decay patterns such as crumbling and spalling were limited in comparison to previous generations
387 (Figure 2). However, salt crusts and salt efflorescence formation were observed for several series. Colour
388 variations exceeding 5 points of ΔL* or ΔE were observed for 3.7, 3.4 and 3.1 series, due to surface loss of
389 material and presence of efflorescence (Figure 7).

390 The weight variation showed trends similar to the second generation, due to salt accumulation and humidity
391 retention due to salt hygroscopicity (Figure 8). In particular 3.1a and 3.1b, 3.5, 3.6 showed loss of material
392 and thick salt crust formation. However, only the conductivity profile of 3.6 (table 3) indicates a higher salt
393 concentration in the external render layer, whilst 3.1 and 3.5 showed quite homogenous profiles. It is
394 possible that a quick salt transport mechanism with deposition of salt only occurred on the external surface.
395 3.2 and 3.7 series had high conductivity in the 10-12 mm range corresponding to the subsurface part, thus
396 indicating storage of salt crystals within the specimens. 3.4 showed an increasing trend of conductivity
397 values from the internal part to the surface.
398 Reduced detachments/delamination were observed under mechanical solicitation by Schmidt Hammer after
399 the cycles (Table 3). 3.2 and 3.7 were more stiff in comparison to the other series, with hammer rebounds
400 higher than 30° for impact stress of 0.88J, possibly also due to the formation of rigid subsurface salt
401 deposition (indicated by conductivity profiles). Values over 20° for impact stress of 0.88J were measured for
402 the other specimens, demonstrating a good balance among stiffness and compactness.
403 Table 4 reports the evaluation of the specimens composing the third generation, rows 22-28.
404

405 **4. Discussion**

406 *4.1 Evolution of the EBN-design across generations and minimization of the degradation features*
407 The evaluations carried out for each generation have allowed us to investigate and model the experimental
408 space. In Figure 9, the evolution of the EBN-design across generations is presented, in particular Figure 9a
409 show the evolution of the mean response function Y and its corresponding standard error . Notably, the mean
410 response decreased from Y=5.03 (sd=2.3) to Y=3.09 (sd=0.87), corresponding to lower decay features and a
411 38% improvement, just in 3 generations of the process. The same behaviour can be observed considering Y_1
412 (detachments) and Y_2 (internal de-cohesion) response variables (Figure 9b), which are the decay features that
413 can cause complete failure of render systems and are responsible for the 40% and 30% respectively of Y, as
414 described in Section 2.2.1. Y_3 (external exfoliations) and in particular Y_4 (efflorescences) usually cause
415 aesthetical damage and not structural collapse, therefore contribute less to the definition of the response
416 function Y and their behaviour reveals this characteristic. In particular in the 3th generation, a homogenous

417 transport of salt solutions to the surface is often observed and the evaporation of water from the external
418 surface leads to crystallization of the salts as innocuous salt efflorescence, avoiding spalling [6-8].
419 Considering all the experimental points ordered by generations, as presented in Figure 10, we can see how
420 the variability of the response decreases. In the first generation, we selected a random sample from the
421 possible specimens, achieving responses with a wide range of values, some of them with response value Y
422 smaller than 3 (4 specimens out of 14, i.e. 28% of the experiments in generation 1). After just 2 generations
423 of the process, we significantly reduced the range of response values in the interval [1.67, 4.32] with 3
424 specimens having response value Y smaller than 3 (i.e. 43% of the experiments in generation 3).
425 Given that our aim was to derive a very small set of informative experimental points with respect to the
426 whole search space, these results seem very good as the EBN-design has a high probability to improve the
427 sustainability and resistance of the renders in the early generations of the design, saving experimental
428 resources and reducing possible waste. Moreover, the approach achieved good values testing just a small set
429 of the whole experimental space, namely less than 26% of the candidate experimental points.
430
431 *4.2 The TAN model after three generations: the probabilistic influence of the composition on the resistance*
432 *to NaCl exposure*
433 The results obtained during the experimentation were used to estimate a TAN model at the end of each
434 generation of the EBN-design process. The TAN model estimated at generation 3 derived by all the tested
435 data of this experimentation, i.e. at the end of the evolutionary procedure, is presented in Figure 11. The class
436 variable represents the target of the optimisation, i.e. the response variable Y, which describes the degree of
437 decay occurred. As required by TAN models, each design variable (recycled aggregate, w/b ratio, water
438 repellent percentage and air entraining percentage) has Y and at most one variable as parents, as indicated by
439 the direct arcs in the network . In this way, we are able to identify the strongest relations amongst the design
440 variables X_i, i=1,…4, with the detrimental effect Y, and how the interconnection network amongst them is
441 developed.
442 It is notable that the type of recycled aggregate is a key factor in the experimentation, as the corresponding
443 variable is parent of all the other variables in the network. This implies that when choosing a specific
444 aggregate, the value of the percentage of water repellent, the water/binder ratio and the percentage of air

445 entraining follow from that assumption. The aggregate type is therefore a significant variable and this needs
446 to be taken into account when using recycled aggregates. In particular, the presence of recycled mortars
447 which are internally water-repellent may have a direct effect on the water transport properties of the first
448 layer, hindering the moisture transport and favouring salt deposition at the interface substrate-first layer, in
449 particular for cement based aggregates (e.g. for mixtures 1.10, 1,11 that had as aggregates CM750 and
450 CMCast containing in turn a 0.5% of water-repellent agent). Whilst the presence of pozzolana or of NHL
451 aggregates may lead to side reactions of the binder, favouring the formation of hydration products and
452 enhancing the strength (e.g. mixtures 1.3, 1.5, 3.2, 3.1 that contains the aggregates PM, NM, NMcast). The
453 effect of the recycled aggregate on the final structure and behaviour, needs to be compensated by the
454 adequate choice of additives and additive dosages, in order to obtain a good durability in the presence of
455 rising damp of salt solutions.
456 When TAN is estimated, we can develop probabilistic inference about design variables, deriving in this way
457 the strength of the relationships among each variable and the decay represented by Y. For example, given
458 that we observed a very low value of Y, say for example included in the interval [1,2), we will derive a
459 probability equal to 0.332 that a specimen is composed by CMcast aggregate. Moreover, conditioned to very
460 low value of Y, the probability of selecting specimens with a water/binder ratio of 1.0 and 1.2 is 0.532 and
461 0.522 respectively, showing that these w/b ratios are equally probable, whilst the aggregate type is not. This
462 confirms the hypothesis that the interconnection network has a key variable in the type of aggregate. In fact,
463 if we condition to a very low value of Y and a CMcast aggregate, we observe with probability equal to 0.896
464 a specimen with water/binder ratio of 1.2. This highlights the very informative role of TAN network in
465 identifying the relationships amongst design variables towards the optimisation problem.
466 *4.2.1 Effect of each composition variable in lowering the global detrimental effect*
467 In order to better visualize the effect of each variable in lowering the global detrimental effect, represented
468 by the answer variable Y, the boxplots of the Y conditioned to each value of the design variables X_i,
469 i=1,…,4, is reported in Figure 12. Boxplots at the top-left present the distribution of Y values, when focusing
470 on a particular recycled aggregate. We can see that whilst NMcast as aggregate produces specimens with
471 value of Y ranging from 3 to 4, CMcast and NM have a wider range of Y values. Whilst the two different
472 values of water/binder ratio produce similar distributions of Y (boxplots at the top-right of Figure 12), it is

clear that using a percentage of air entraining equal to 0.09% produces in average low values of the response (boxplots at the bottom-left of Figure 12). This behaviour can be explained by considering previous researches that highlighted the effects of air-entraining agents, such as porosity increase, formation of larger pores able to host large amount of salts prior to suffering detrimental effects, better interconnection of the substrate with the porous structure of the render layer and enhanced moisture transport, [5~~6~~7-5~~7~~8]. Concerning the percentage of water repellent, whilst there are no statistically significant differences in the distributions of Y when conditioning on 0.00% and 0.30% values, there is an increase of the median response value when considering 0.50% of water repellent. The use of high percentages of water repellents in presence of rising damp is known to have hindering effect of the liquid flux [38, 47]. This often leads to the recession of the evaporation front within the render layer, causing salt deposition within the layer and subsequently the sub-efflorescences formation and delamination. Despite this drawback when using the water repellent admixture, the experiment demonstrated that with low dosages, the internal salt solution flux is adequately regulated, whilst the protection against the entrance of external water is assured.

Focusing on the percentage of air entraining for which there is a clear difference in the response behaviour when conditioning on the two possible values, we notice that in Figure 13, when combined with a particular aggregate, the reduced percentage of the air entraining (0.03%) could provide a positive effect. For example, a specimen composed by the CMcast aggregate mixed at a 0.03% of air entraining, most of time leads to a response value Y in the optimality area of the experimentation, apart from one which has response Y=10 (ID experiment 2.3 of the second generation). To understand what could affect this experiment, we notice that this is the only mixture in which there is a percentage of water repellent equal to 0.5%, subsequently failure occurred due to preferential salt deposition within the first layer, delamination and detachment. A similar trend can be observed for NMcast, with higher value of Y with 0.03% of water repellent being associated with a 0.5% of water repellent in the external layer. When we consider mixtures added with NM, the use of 0.09% of air entraining agent is necessary to observe good durability, independently from the water-repellent's percentage of the external layer,the air entraining admixture possibly regulates the first layer's structure, allowing a good equilibrium of salt transport or storage during the cycles (as in 3.1).

5 Conclusions

Comment [LF6]: * At the conclusions, the authors should highlight the methodology final purpose and outcomes. To help building practitioners or managers? To support designers, manufacturers or experts?

The development of render systems able to endure in presence of salt solution and masonries contaminated by salts is still an open challenge for designers and manufacturers that often involves high research costs.

The methodology applied in this study, effectively addressed the main goal of enhancing the durability of render systems exposed to the absorption/drying cycles of NaCl solution, by optimizing their compositions. Three generations were developed in order to obtain a significant reduction of the observed degradation forms, testing only 28 of experimental points out of 108 possible candidates.

The procedure, developed across three sequential generations, allows to prepare and test 7 systems at a time (28 specimens), that can be easily managed even in small and medium sized laboratories with low costs. However, critical points were:

- the repetition of the procedure for each generation that requires long research times (1 month for the specimens preparation and 1 month for the exposure and evaluation). Therefore, it is particularly important to reach a significant optimization in few generations, as in our case;
- the definition of the response Y. We choose to define our target as a weighted sum of several decay features. The weights were chosen on the basis of the severity of the decay forms, as commonly considered in the conservation field (i.e. complete detachment over de-cohesion over external crumbling over surface efflorescence);
- the evaluation of the degradation forms. The subjective nature of the "mark" influences the evolution of the design process and the achieved results. In order t~~Thus,~~o limit the subjectivity, the marks are given by an expert researcher that integrates the impressions obtained by ~~a~~ visual observation of the decay extension and severity ~~level~~ for each specimen ~~was integrated by~~with the results of quantitative measures of physical behavior (weight and colour variations, flexibility, location of salts) .

The results highlighted that:

- the resistance to salt crystallization, tested by absorption and drying cycles of NaCl solution as defined in [8], depends particularly on the correct use of water-repellent and air-entraining agents.
- Air-entraining dosage of 0.09% is suggested.
- Lower dosages of water-repellent (0% or 0.3%) reduce the degradation phenomena, possibly allowing the solution flux till the surface and advection transport of salts.

Comment [LF7]: Thus, a visual observation of the decay extension and severity level for each specimen was integrated by the results of quantitative measures of physical behavior (weight and colour variations, flexibility, location of salts)." - This sentence is not clear. It may be simply a language issue

Comment [LF8]: - I would suggest using "resistance to salt crystallization" instead of simply "resistance" and adding some information about how that resistance was evaluated. The sentence would become something like "The resistance to salt crystallization, as defined by ????, depends…"

- The recycled aggregate type did not show univocal trend and its effect must be considered in association with the other variables. The use of cement-based aggregates containing water repellents (CM750, CMcast) in association with 0,09% air entraining dosage diminished the render adhesion to the brick and did not enhance the systems durability, whilst, the use of NHL-based aggregates (NM, NM750, NMcast) with 0.09% air entraining content gave good results, most likely due to good compatibility between aggregates and the NHL binder.

In order to better understand the renders effectiveness, the authors have envisaged further research addressing the study of the transport mechanisms and salt depositions within the systems, based on the investigation of the double layer microstructure, porosity and properties such as water absorption or drying behavior. Moreover, future prospects foresee the application of the optimized system in meso scale models and on real historical masonries. The future testing should definitely confirm the renders suitability, however the results already obtained are promising for further application of this statistic methodology on a larger scale in order to optimize the render design reducing the research costs for the advantage of manufacturers and guarantying render effectiveness and compatibility for users satisfaction.

Acknowledgments

The Authors acknowledge Ca' Foscari Universtiy, DAIS department for funding the two-year grant "Physical degradation of historical masonries subjected to rising damp and remediation methods", the JPI EMERISDA Project "Effectiveness of Methods against Rising Damp in Buildings" and VICCS-UNIVE for funding a one-year grant "Impatto dei cambiamenti climatici sulle superfici architettoniche in ambiente Venezia" .
The authors want to thank Jade Straker for her linguistic support.

References

[1] B. Lubelli, R.P.J. Van Hees, C.J.W.P. Groot, Sodium chloride crystallization in a "salt transporting" restoration plaster, Cem.ConcreteRes. 36-8 (2006)1467–1474.
[2] B. Lubelli, R.P.I. Van Hees, H.P. Huinink, C.J.W.P. Groot, Irreversible dilation of NaCl contaminated lime–cement mortar due to crystallization cycles, Cem.ConcreteRes. 36-4 (2006) 678–687.
[3] B. Lubelli, M.R. de Rooij, NaCl crystallization in restoration plasters, Constr.Build.Mater 23 (2009) 1736–1742.
[4] T. Diaz Gonçalves, Salt crystallization in plastered or rendered walls, PhD thesis supervisor Delgado Rodrigues J, Universidade Técnica de Lisboa, Lisbon, 2007.
[5] G.W. Scherer , Stress from crystallization of salt in pores, in: 9th International Congress on Deterioration and Conservation of Stone, Venice, 2000.
[6] J. Petkovic´, H.P. Huinink, L. Pel, K. Kopinga, R.P.J. van Hees, Salt transport in plaster/substrate layers, Mater Struct 40 (2007) 475–490.
[7] J. Petkovic ´,H.P. Huinink, L .Pel, K. Kopinga, R.P.J. van Hees, Moisture and salt transport in three-layer plaster/substrate systems, Constr .Build. Mater. 24 (2010) 118–127.
[8] T. Wijffels, B. Lubelli, Development of a new accelerated salt crystallization test, in: Special Issue: COMPASS, Heron Journal 51-1 (2006), http://heronjournal.nl/51-1/2006_1.html
[9] Fragata, M. Rosário Veiga, A. Velosa, Substitution ventilated render systems for historic masonry: Salt crystallization tests evaluation, Constr. Build. Mater. 102- 1 (2016) 592-600.
[10] Groot, R. van Hees, T. Wijffels, Selection of plasters and renders for salt laden masonry substrates, Constr.Build.Mater 23-5 (2009) 1743–1750.

[11] M.A. Karoglou,A. Bakolas, N. Kouloumbi, A. Moropoulou, Reverse engineering methodology for studying historic buildings coatings: The case study of the Hellenic Parliament neoclassical building, Prog.Org.Coat. 72/ 1–2 (2011) 202-209.
[12] The Cement Sustainability Initiative (CSI), reports for http://www.wbcsdcement.org/ 2015 (accessed 12.12.2015).
[13] L. Barcelo, J. Kline, G. Walenta, E. Gartner, Cement and carbon emissions, Mater.Struct. 47 (2014) 1055–1065.
[14] Gulotta D., Goidanich S., Tedeschi C., Nijland T.G., Toniolo L., Commercial NHL-containing mortars for the preservation of historical architecture. Part 1: Compositional and mechanical characterisation, Construction and Building Materials 38 (2013) 31–42
[15] M. Stefanidou, E. Anastasiou, K. Georgiadis Filikas, Recycled sand in lime-based mortars, Waste Manage 34 (2014) 2595–2602.
[16] R. Raeis Samiei, B. Daniotti, R. Pelosato, G. Dotelli, Properties of cement–lime mortars vs. cement mortars containing recycled concrete aggregates, Constr.Build.Mater. 84 (2015) 84–94.
[17] JR Jiménez, J Ayuso, M López, JM Fernández, J De Brito Use of fine recycled aggregates from ceramic waste in masonry mortar manufacturing, , Construction and Building Materials 40 (2013) 679-690
[18] M Braga, J De Brito, R Veiga, Incorporation of fine concrete aggregates in mortars, Construction and Building Materials 36 (2012) 960-968
[19] P. Saiz Martínez, M. González Cortina, F. Fernández Martínez, A. Rodríguez Sánchez, Comparative study of three types of fine recycled aggregates from construction and demolition waste (cdw), and their use in masonry mortar fabrication, J.Clean.Prod. 118 (2016) 162-169.
[20] L. Senff, D. Hotza, W. L. Repette, V. M. Ferreira, J. A. Labrincha, Influence of added nanosilica and/or silica fume on fresh and hardened properties of mortars and cement pastes, Adv.Appl.Ceram.108-7 (2009) 418-428.
[21] R. Zaitri, M. Bederina, T. Bouziani, Z. Makhloufi, M. Hadjoudja, Development of high performances concrete based on the addition of grinded dune sand and limestone rock using the mixture design modelling approach, Constr. Build. Mater. 60 (2014) 8–16.
[22] Schackow, C. Effting, M. V. Folgueras, S. Güths, G. A. Mendes, Mechanical and thermal properties of lightweight concretes with vermiculite and EPS using air-entraining agent, Constr. Build. Mater. 57 (2014) 190–197.
[23] M.C.S. Ribeiroa, A. Fiúza, A.C.M. Castro, F.G. Silva, M.L. Dinis, J.P. Meixedo, M.R. Alvim, Mix design process of polyester polymer mortars modified with recycled GFRP waste materials, Compos.Struct. 105 (2013) 300–310.
[24] V. Ferrándiz-Mas,L.A.Sarabia,M.C.Ortiz, C.R. Cheeseman, E. García-Alcocel, Design of bespoke lightweight cement mortars containing waste expanded polystyrene by experimental statistical methods, Mater.Design 89 (2016) 901–912.
[25] R. Baragona, F. Battaglia, I. Poli Evolutionary statistical procedures, 2011, Springer-Verlag, Berlin.
[26] D. Slanzi, I. Poli, Evolutionary Bayesian network design for high dimensional experiments, Chemometr. Intell. Lab. 135 (2014) 172–182.
[27] D. Slanzi, D. De Lucrezia, I. Poli, Querying Bayesian Networks to design experiments with application to 1AGY serine esterase protein engineering, Chemometr. Intell. Lab. 149, Part A (2015) 28-38.
[28] M. Borrotti, D. De March, D. Slanzi, I. Poli, Designing lead optimisation of mmp-12 inhibitors, Comput. Math. Method. M., vol 2014(2014)1-8.
[29] J. Pearl, Probabilistic Reasoning in Intelligent Systems: Networks of Plausible Inference. Morgan Kaufmann, 1998.
[30] R.G. Cowell, A.P. Dawid, S.L. Lauritzen, D.J. Spiegelhalter, Probabilistic Networks and Expert Systems. Springer-Verlag, 1999.
[31] D. Koller, N. Friedman, Probabilistic graphical models: principles and techniques — adaptive computation and machine learning, The MIT Press, 2009.
[32] K. Korb, A. Nicholson, Bayesian Artificial Intelligence. Chapman & Hall/CRC, 2010.
[33] M. Scutari, J. Denis, Bayesian networks: with examples in R, Chapman & Hall/CRC Texts in Statistical Science, Taylor & Francis, 2014.
[34] M. Forlin; D. Slanzi; I. Poli, Combining Probabilistic Dependency Models and Particle Swarm Optimization for Parameter Inference in Stochastic Biological Systems. In: FL Gaol, QV Nguyen (Eds), Proceedings of the 2011 2nd International Congress on Computer Applications and Computational Science, Springer, vol. 145 (2012) 437-443.
[35] M. Borrotti, I. Poli, Nave bayes ant colony optimization for experimental design. In: R. Kruse, M.R. Berthold, C. Moewes, M.n. Gil, P. Grzegorzewski, O. Hryniewicz (Eds.), Synergies of Soft Computing and Statistics for Intelligent Data Analysis, Vol. 190 of Advances in Intelligent Systems and Computing, Springer, Berlin Heidelberg (2013) 489–497.
[36] J. Lanas, P. Bernal, M.A. Bello, A. Galindo, Mechanical properties of natural hydraulic lime-based mortars. Cem Concrete Res. 34-12 (2004) 2191-2201.
[37] B.A. Silva, A.P. Ferreira Pinto, A. Gomes, Natural hydraulic lime versus cement for blended lime mortars for restoration works, Constr.. Build.Mater. 94 (2015) 346–360.
[38] L. Falchi, U. Müller, P. Fontana, F.C. Izzo, E. Zendri, Influence and effectiveness of water-repellent admixtures on pozzolana–lime mortars for restoration application, Constr. Build. Mater. 49 (2013) 272–280.

[39] M. Lanzón, P.A. Garcia Ruiz, Effectiveness and durability evaluation of rendering mortars made with metallic soaps and powdered silicone, Constr Build Mater 22 (2008) 2308-2315.
[40] L Falchi, C Varin, G Toscano, E Zendri, Statistical analysis of the physical properties and durability of water-repellent mortars made with limestone cement, natural hydraulic lime and pozzolana-lime. Constr. Build.Mater. 78(2015) 260–270.
[41] P.L. Gaspar, J. de Brito, Quantifying environmental effects on cement-rendered facades: A comparison between different degradation indicators, Build.Environ. 43 (2008) 1818–1828.
[42] J. Delgado Rodrigues, A. Grossi, Indicators and ratings for the compatibility assessment of conservation actions, J.Cult.Herit. 8 (2007) 32-43.
[43] J.Grilo, A Santos Silva., P.Faria, A.Gameiro, R. Veiga, A. Velosa, Mechanical and mineralogical properties of natural hydraulic lime-metakaolin mortars in different curing conditions, Construction and Building Materials 51 (2014) 287–294
[44] S. Barr, W.J. Mc Carter,B. Suryanto, Bond strenght performance of hydraulic lime and natural cement mortared sandstone masonry, Construction and Building materials 84 (2015) 128-135
[45] M.P. Seabra, J.A. Labrincha, V.M. Ferreira, Rheological behaviour of hydraulic lime-based mortars, Journal of the European Ceramic Society 27 (2007) 1735–1741
[46] G. Cultrone, E. Sebastia ´n, M. Ortega Huertas, Forced and natural carbonation of lime-based mortars with and without additives: Mineralogical and textural changes, Cement and Concrete Research 35 (2005) 2278 – 2289
[47] T. Zhao, F.H. Wittman, R. Jiang, W. Li, Application of silane-based compounds for the production of integral water repellent concrete, in: E.Borelli, V.Fassina (Eds.), Proceedings of Hydrophobe VI, 6th international conference on water repellent treatment of building materials, Aedificatio Publisher, Freiburg, 2011, pp 137-144.
[48] L. Falchi,E. Zendri, E. Capovilla, P. Romagnoni, M. De Bei., The behaviour of water-repellent mortars with regards to salt crystallization: from mortar specimens to masonry/render systems, Mater Struct (2017) 50: 66.
[49] UNI8941:1987 coloured surface- colorimetry, principles, colour measurement, calculation of colour differences
~~[49]~~[50] Schmidt OS-120PT, information illustrating the device and its use available at: https://www.proceq.com/compare/schmidt-rebound-hammers/; https://www.proceq.com/uploads/tx_proceqproductcms/import_data/files/Schmidt%20OS-120_Operating%20Instructions_English_high.pdf; https://youtu.be/wZOuJ7L5ojI; (last access 14/03/2017).
~~[50]~~[51] Normal 13/83 Dosaggio dei Sali solubili totali mediante misure di conducibilità (italian normative on stone material- determination of the content of soluble salts with conductivity measurments) 1983.
~~[51]~~[52] J.B.O Mitchell, Machine learning methods in chemoinformatics. Wiley Interdisciplinary Reviews: Computational Molecular Science, 4-5(2014) 468-481.
~~[52]~~[53] M. Ramoni, P. Sebastiani, Robust Bayes classifiers, Artiff. Intell., 125-1 (2001) 209–226.
~~[53]~~[54] N. Friedman, D. Geiger, M. Goldszmidt, Bayesian Network Classifiers, Mach. Learn., 29-2/3 (1997) 131-163.
~~[54]~~[55] C. Bielza, P. Larrañaga, Discrete bayesian network classifiers: A survey. ACM Comput. Surv., 47-1 (2014), nr 5.
~~[55]~~[56] The R Project for Statistical Computing. www.r-project.org
~~[56]~~[57] H.F.W. Taylor, Cement Chemistry, Second ed., Academic press, London, 1997.
~~[57]~~[58] H.N. Atahan, C. Carlos Jr., S. Chae, P.J.M. Monteiro, J. Bastacky, The morphology of entrained air voids in hardened cement paste generated with different anionic surfactants, Cement Concrete Comp. 30-7 (2008) 566-575.

Formatted: Comment Text
Formatted: English (United States)
Formatted: Font: Times New Roman, English (United States)
Field Code Changed
Formatted: Font: Times New Roman, English (United States)
Formatted: Font: Times New Roman, English (United States)
Formatted: Default Paragraph Font
Formatted: English (United States)

Optimization of sustainable, NaCl-resistant and water-repellent renders through evolutionary experimental design

Laura Falchi[a*], Debora Slanzi[a, b], Laura Speri, Irene Poli [a, b], Elisabetta Zendri[a]

[a]Department of Environmental Sciences, Informatics and Statistics, Ca' Foscari University of Venice

[b]ECLT, European Centre for Living Technology

Tables and Table captions

Table 1. General composition of the specimens

Layer	Dimension	Name	Description	Proportion
Substrate	16cm X 12cm X 2cm	*Red brick*	Full red clays bricks	
First render layer	16cm X 12 cm X 0.75 cm	*NHL*	Natural hydraulic lime binder, NHL3.5	1 part by volume
		Sand	Siliceous, limestone sand (size fraction 0/5 mm)	2 parts by volume
		Recycled mortars		
		CM	Limestone cement mortar without admixtures	1 part by volume
		CM750	Limestone cement mortar with 0.5% of siloxane Sitren P750	
		CMcast	Limestone cement mortar with 0.5% of Calcium stearates	
		PM	Pozzolana-lime mortar without admixtures	
		PM750	Pozzolana-lime mortar with 0.5% of siloxane Sitren P750	
		PMcast	Pozzolana-lime mortar with 0.5% of calcium stearates	
		NM	Natural hydraulic lime mortar without admixtures	
		NM750	Natural hydraulic lime mortar with 0.5% of Sitren P750	
		NMcast	Natural hydraulic lime mortar with 0.5% of calcium stearates	
		Hostapur	Air entraining agent, lignin sulfonate	0.03%; 0.09%w/w_b
		Water	Tap water	w/b 1.0; 1.2
Second render layer	16 cm X 12 cm X 0.5 cm	*NHL*	Binder, natural hydraulic lime NHL3.5	2 part by volume
		Sand	Siliceous, carbonate sand (size fraction 0/2 mm)	3 parts by volume
		Water repellent admixtures		0%; 0.3%; 0.5%w/w_b
		P750	Silane-siloxane supported on a silica carrier	
		Cast	Calcium stearates technical grade	
		water	Tap water	w/b 1.0

*W_b= binder weight; w/b=water-binder ratio

Table 2 . Specimen compositions of the three-generations investigated

	ID exps Render system	First layer			Second layer
		X_1 Recycled aggregate	X_2 w/b	X_3 Air entraining %	X_4 Water repellent%
1st Generation	1.1	NMcast	1.2	0.09%	0.0%
	1.2	PMcast	1.0	0.03%	0.3%
	1.3	PM	1.2	0.03%	0.3%
	1.4	CMcast	1.0	0.03%	0.0%
	1.5	NM	1.2	0.09%	0.5%
	1.6	PM750	1.0	0.03%	0.5%
	1.7	CMcast	1.2	0.03%	0.3%
	1.8	CM	1.0	0.03%	0.0%
	1.9	CM750	1.2	0.09%	0.5%
	1.10	CM750	1.0	0.03%	0.0%
	1.11	CMcast	1.0	0.09%	0.3%
	1.12	NM	1.0	0.03%	0.3%
	1.13	NM750	1.0	0.03%	0.3%
	1.14	NM750	1.2	0.03%	0.5%
2nd Generation	2.1	CMcast	1,00	0.03%	0.3%
	2.2	CMcast	1,20	0.03%	0%
	2.3	CMcast	1,20	0.03%	0.5%
	2.4	PMcast	1,00	0.03%	0.5%
	2.5	PMcast	1,20	0.03%	0.3%
	2.6	NM	1,20	0.03%	0.5%
	2.7	NM	1,00	0.09%	0.3%
3rd Generation	3.1	NM	1.0	0.09%	0%
	3.2	NMcast	1.0	0.09%	0.3%
	3.3	NMcast	1.0	0.03%	0.3%
	3.4	NM750	1.2	0.09%	0%
	3.5	CM	1.2	0.09%	0%
	3.6	CM	1.2	0.03%	0.5%
	3.7	PM750	1.0	0.09%	0.3%

Table 3. Sclerometric measurements: the mean of three specimens is reported for a percussion strength of 0.44J and for 0.88J, together with the indication of the detachment during this measurement; Conductivity profile measured on the mortar layer after the cycle (≤90 μs/cm = light gray; 90-130 μs/cm =gray; 131-150 μs/cm=medium gray; ≥150 μs/cm dark gray) .

	Render system	**Nr. specimens detached before exposure***	**Sclerometric rebound**			**Nr specimens detached after sclerometer**	**Conductivity profile (μs/cm) Int. →ext**			
			0.44J Mean ± dev.st	0.88J Mean ± dev.st	Average nr of strikes for **detached** specimens		1st Layer		2nd Layer	
							0-4 mm	5-9 mm	10-12 mm	13-15 mm
1st Generation	1.1	2/3	8.0±1.5	12,9±9,0	7	2/3	107,7	94,4	196,6	176,2
	1.2	-	12,6±2,2	19,2±9,7	6	3/3	105,0	108,3	114,6	134,4
	1.3	2/3	9,1±1,6	14,5±1,0	7	3/3	116,7	115,2	138,7	163,0
	1.4	-	7,9±1,7	9,4±2,0	6	3/3	90,8	98,7	110,2	149,6
	1.5	-	8,3±2,3	9,4±2,4	-	-	91,5	107,7	109,0	394,5
	1.6	2/3	9,7±2,3	10,6±2,1	7	3/3	61,4	75,3	96,0	153,7
	1.7	-	7,5±0,8	10,1±1,8	-	-	97,8	87,8	168,2	148,8
	1.8	2/3	5,8±5,0	15,3±5,3	-	2/3	101,5	75,2	84,5	127,9
	1.9	1/3	6,6±2,7	24,7±7,6	9	3/3	88,7	85,8	116,8	171,1
	1.10	2/3	11,4±4,8	15,5±3,5	7	3/3	90,3	72,1	86,3	171,6
	1.11	2/3	6,0±3,3	x	4	3/3	141,5	101,7	204,2	x
	1.12	3/3	x	x	x	x	x	x	x	x
	1.13	1/3	4,5±2,2	29,7±5,7	-	1/3	77,0	75,4	94,3	184,0
	1.14	2/3	13,0±6,7	21,7±4,6	9	3/3	96,9	85,1	100,2	288,1
2nd Generation	2.1	-	9,8±1,5	19,6±3,4	8	2/3	120,0	100,7	148,0	109,4
	2.2	1/3	8,4±2,5	21,4±6,2	9	2/3	99,7	105,9	112,4	153,2
	2.3	3/3	x	x	x	x	x	x	x	x
	2.4	2/3	8,6±1,5	24,0±4,3	-	2/3	95,9	91,4	88,8	133,0
	2.5	2/3	7,4±1,7	20,6±7,4	9	3/3	100,1	104,5	94,5	158,5
	2.6	1/3	7,7±3,1	20,2±5,4	-	1/3	139,4	81,6	79,6	174,2
	2.7	1/3	8,8±2,5	25,3±5,1	9	2/3	77,7	83,9	138,8	151,1
3rd Generation	3.1	-	12,9±2,3	29,6±7,1	-	-	148,6	138,7	127,5	134,7
	3.2	-	12,5±3,1	34,6±4,4	7	2/3	88,5	149,0	242,2	139,8
	3.3	1/3	9,7±3,8	26,2±3,9	-	1/3	107,3	114,2	137,5	174,5
	3.4	-	9,5±2,5	20,1±7,1	8	2/3	81,5	77,4	116,3	125,0
	3.5	-	9,5±1,6	22,9±8,5	5	1/3	99,2	119,6	100,4	124,9
	3.6	-	10,1±3,4	23,7±6,3	7	2/3	96,2	98,8	127,2	145,6
	3.7	-	10,7±2,6	35,4±7,6	8	1/3	90,1	110,5	196,1	123,3

-= no detachment; x=complete detachment or erosion: no possible measurement

* some mortars/renders were detached from the brick substrate before the salt cycles and therefore were not tested

Table 4. marks the first generation, 10=completely present; 1=not present.
Y_1= bodily detachments; Y_2=internal de-cohesion and crumbling, Y_3=external erosion/exfoliation and crypto efflorescences, Y_4=external efflorescences

	Render system	Y_1	Y_2	Y_3	Y_4	Y
1st Generation	1.1	6,00	4,00	1,00	1,00	3,90
	1.2	2,00	2,00	4,00	5,00	2,70
	1.3	6,00	5,00	3,00	2,00	4,70
	1.4	2,00	2,00	2,00	3,00	2,10
	1.5	1,00	2,00	4,00	3,00	2,10
	1.6	6,00	10,00	9,00	4,00	7,60
	1.7	1,00	2,00	1,00	5,00	1,70
	1.8	7,00	5,00	4,00	10,00	6,10
	1.9	5,00	7,00	4,50	7,00	5,70
	1.10	8,00	7,00	4,00	4,00	6,50
	1.11	9,00	5,00	2,00	3,00	5,80
	1.12	10,00	x	x	x	10,00
	1.13	4,00	8,00	4,00	3,00	5,10
	1.14	7,67	8,00	3,00	4,00	6,47
2nd Generation	2.1	2,00	5,33	4,00	5,67	3,77
	2.2	4,00	1,00	2,00	1,50	2,45
	2.3	10,00	x	x	x	10.00
	2.4	7,67	7,00	9,00	8,00	7,77
	2.5	7,33	6,00	4,00	8,00	6,33
	2.6	5,00	7,00	6,50	5,00	5,90
	2.7	4,00	2,50	3,50	8,00	3,85
3rd Generation	3.1	1,00	2,00	2,00	2,67	1,67
	3.2	2,00	3,00	4,33	7,67	3,33
	3.3	3,67	2,50	7,00	7,00	4,32
	3.4	2,67	3,33	6,00	4,67	3,73
	3.5	2,33	1,00	2,00	7,33	2,37
	3.6	3,33	2,67	2,67	6,67	3,33
	3.7	3,00	3,00	2,33	3,00	2,87

x= complete detachment before the cycle occurred

Optimization of sustainable, NaCl-resistant and water-repellent renders through evolutionary experimental design

Laura Falchi[a*], Debora Slanzi[a, b], Laura Speri, Irene Poli [a, b], Elisabetta Zendri[a]

[a]Department of Environmental Sciences, Informatics and Statistics, Ca' Foscari University of Venice

[b]ECLT, European Centre for Living Technology

Figure Captions

Figure 1. Structure of the render-brick system, two layers of render with composition, indicated by the experimental design, were applied on a full brick, resembling the historical bricks used in Venice.

Figure 2. Scans of some of the representative specimens before and after the crystallization cycles. The specimens demonstrate the major degradation forms and relative severity observed. Group i) complete detachment before the cycles (1.8b as 1.12, 2.3); ii) efflorescences without substantial loss of material (3.1c as 1.1, 2.1, 2.3,.3.2), iii) slight darkening of the surfaces due to the presence of hygroscopic salts (1.7 similar to 2.7); iv) diffuse presence of efflorescence and/or diffuse darkening of the surfaces (1.2 similar to 1.3, 1.4, 1.11, 2.6); v) presence of surface delamination without internal de-cohesion (1.13 similar to 1.14,1.5); vi, vii) diffuse delamination and spalling with internal decohesion (es 3.4 similar to 1.6, 1.8, 1.9, 1.10, 2.4, 2.5, 3.1a and b, 3.5, 3.6, 3.3); vii) limited presence of surface de1amination but the presence of subefflorescence and reduced internal de-cohesion (3.7 similar to 2.2) .

Figure 3. Absolute lightness variation ΔL^* and total colour variation ΔE with specular component included in the first generation. The whole set 1.12 was not measured, as the specimens detached before the exposure.

Figure 4. Weight variation during the exposure measured on dried specimens from the first generation at each cycle

Figure 5. Absolute lightness variation ΔL^* and total colour variation ΔE with specular component included in the second generation.

Figure 6. Weight variation during the exposure measured on dried specimens from the second generation at each cycle

Figure 7. Absolute lightness variation ΔL^* and total colour variation ΔE with specular component included in the third generation.

Figure 8. Weight variation during the exposure measured on dried specimens from the third generation at each cycle

Figure 9. The evolution across generations of the mean response function Y representing the target of the optimization (a) and of the mean response variables Y_i, i=1,…,4 representing the selected parameters of decay (b)

Figure 10. EBN-design response values ordered by generations. The ID experimental point of specimens with response function Y smaller than 3 is reported.

Figure 11. The TAN model estimated at the end of the EBN-design process.

Figure 12. The boxplots of the response variable Y conditioned to each value of the design variables X_i, i=1,…,4

Figure 13. The dotplot of the response variable Y conditioned to recycled aggregate and percentage of air entraining.

Figure 1

Click here to download high resolution image

Figure 2

Click here to download high resolution image

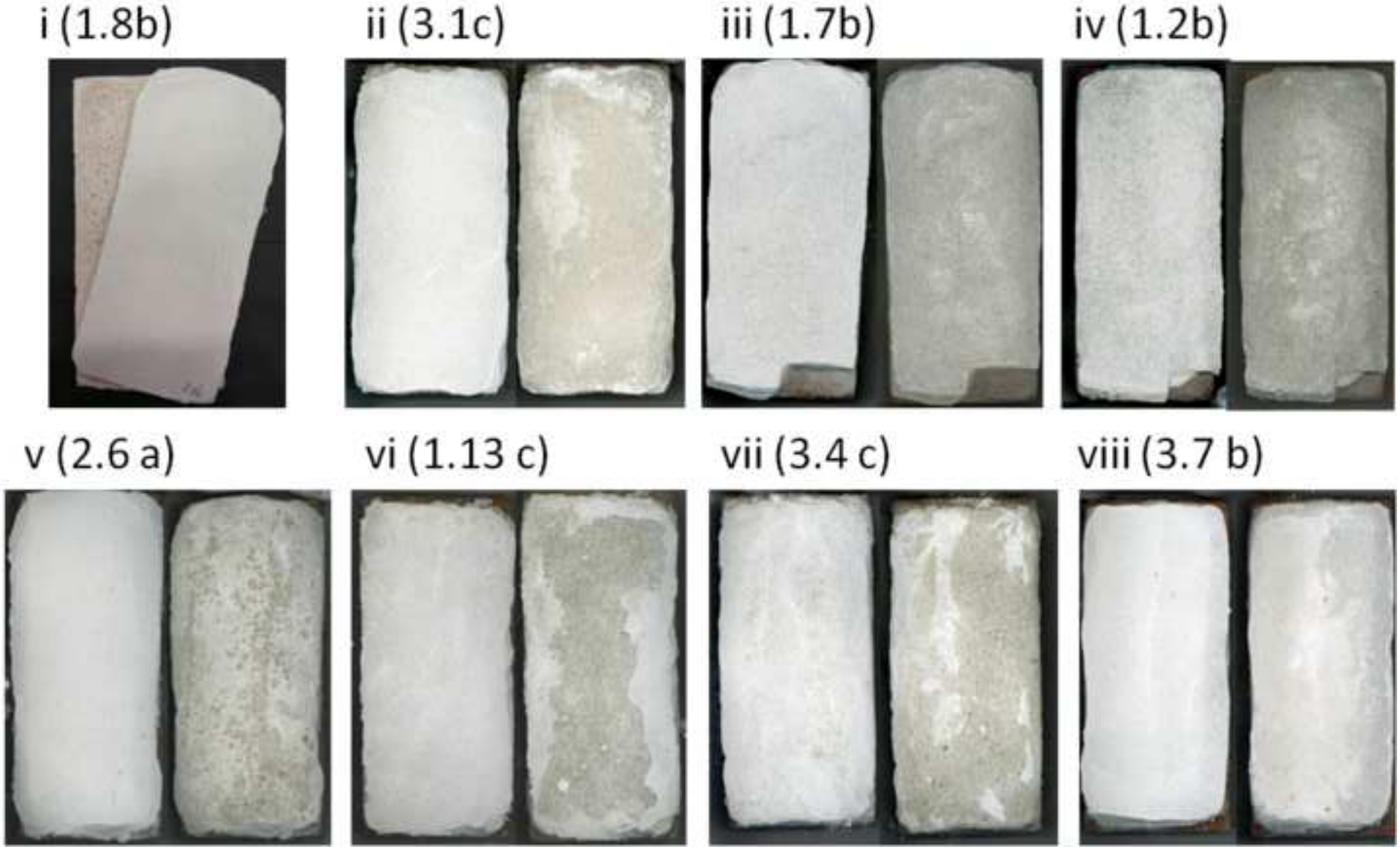

Figure 3

Click here to download high resolution image

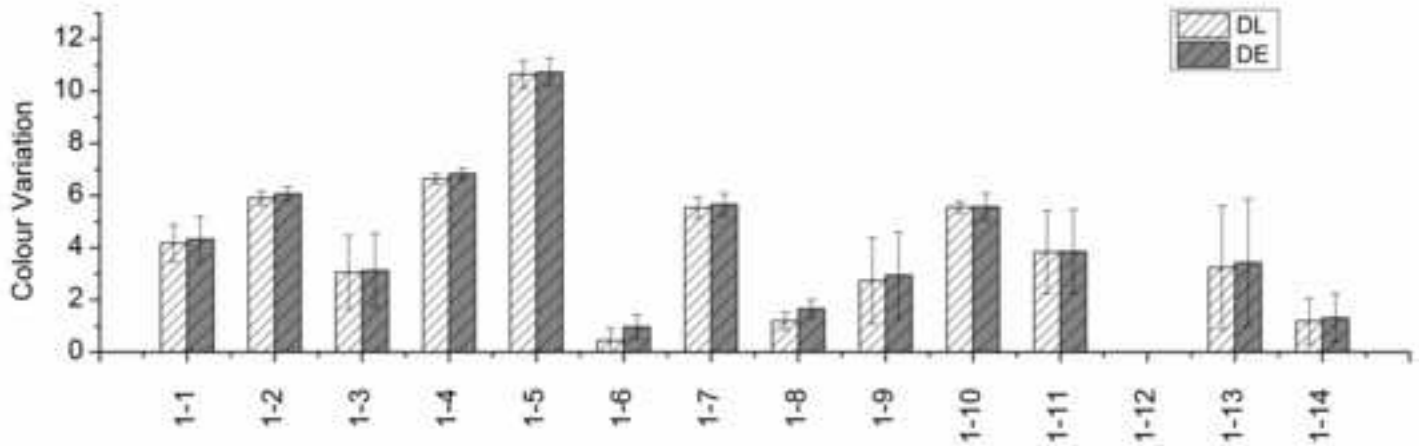

Figure 4

Click here to download high resolution image

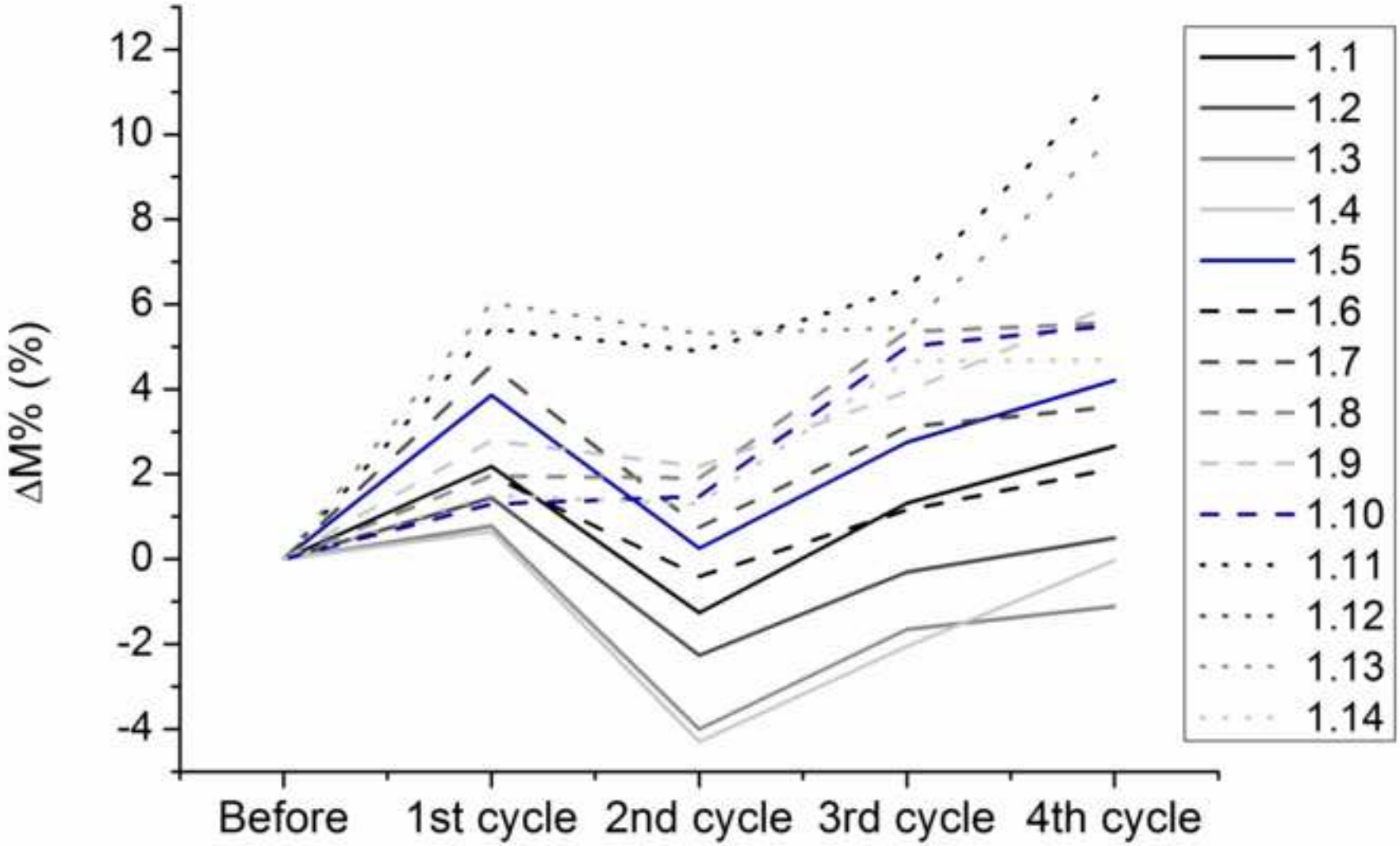

Figure 5

Click here to download high resolution image

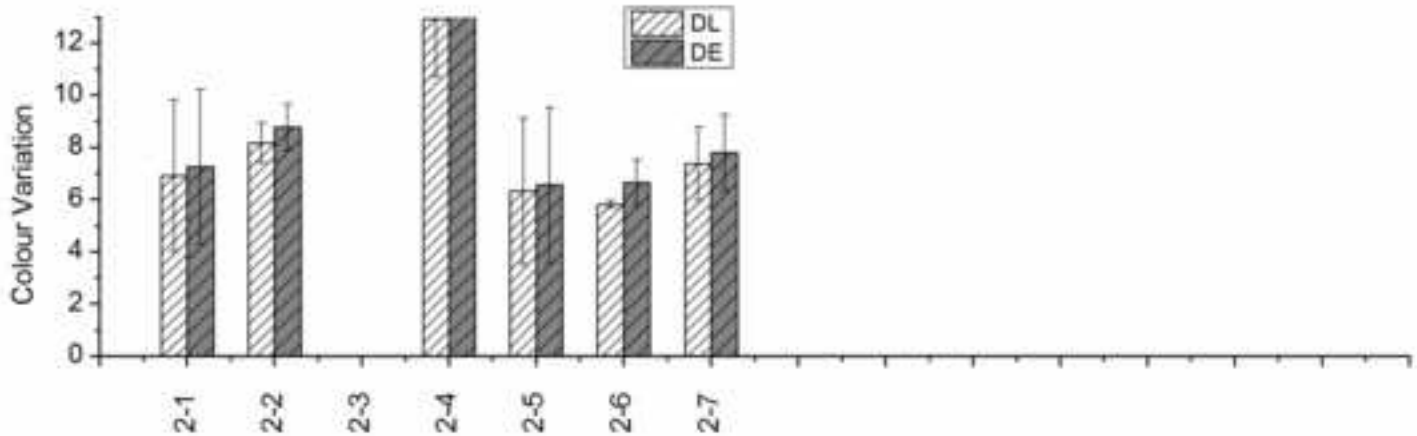

Figure 6

Click here to download high resolution image

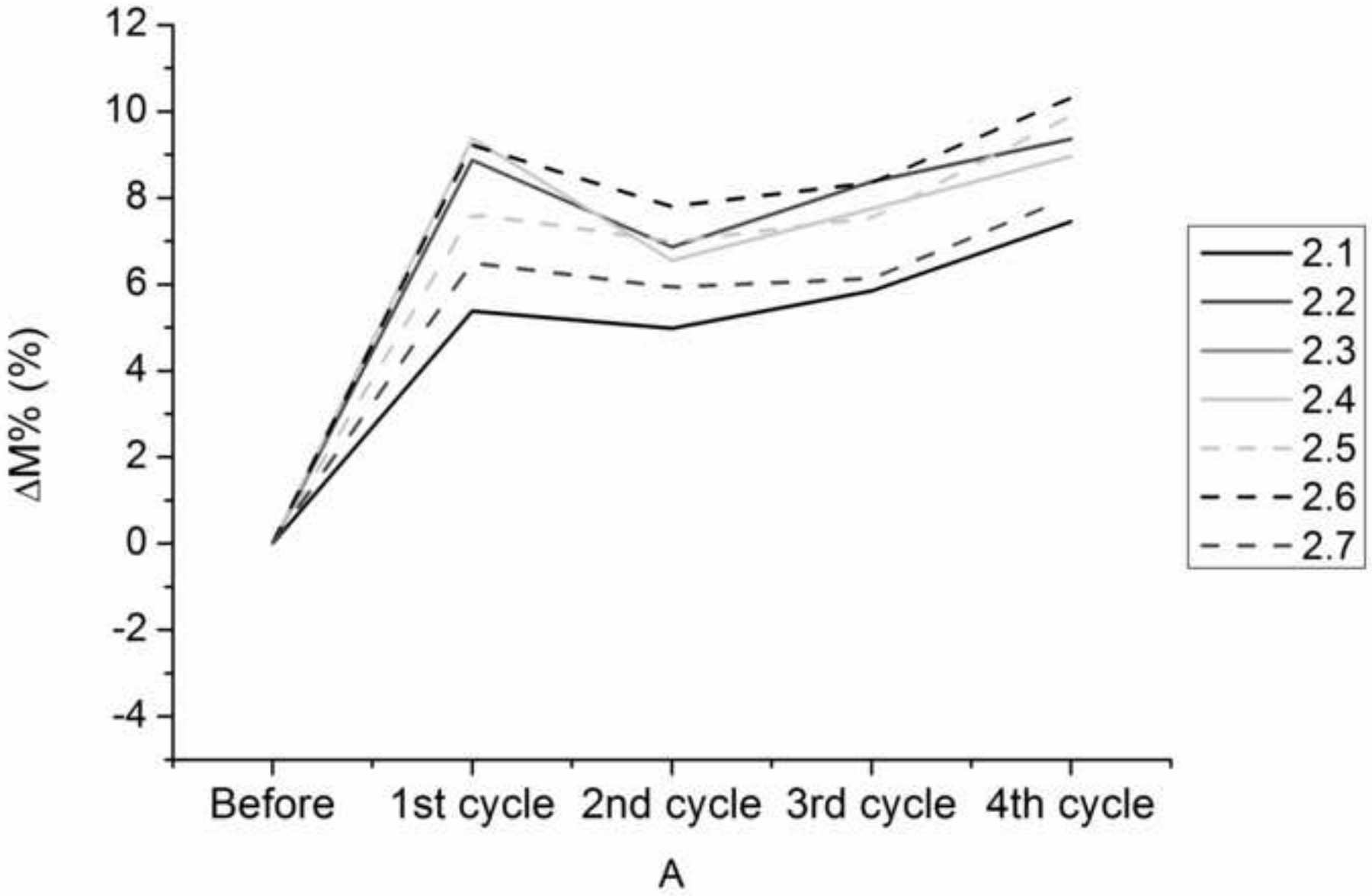

Figure 7

Click here to download high resolution image

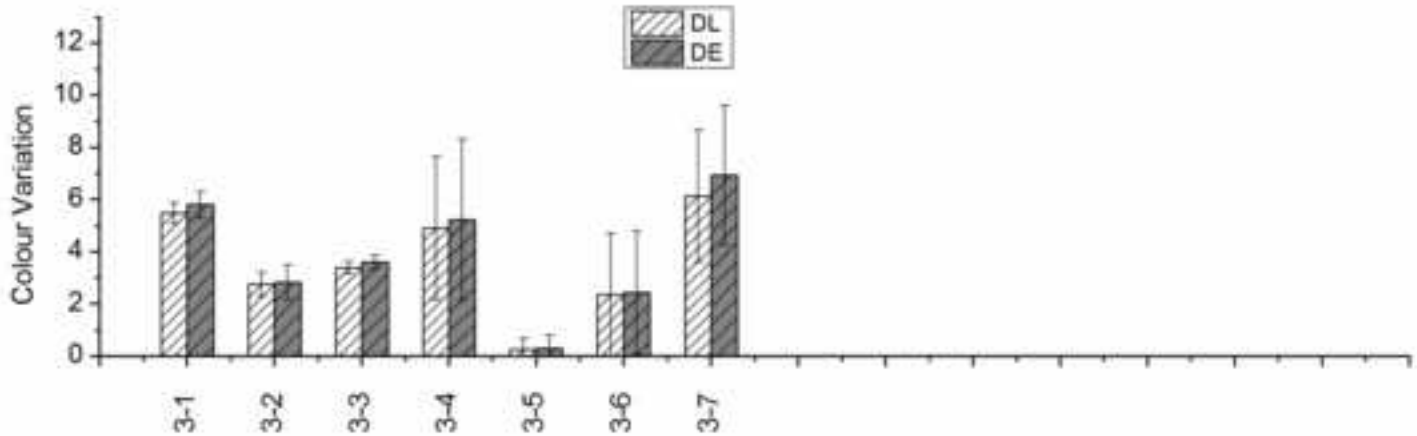

Figure 8

Click here to download high resolution image

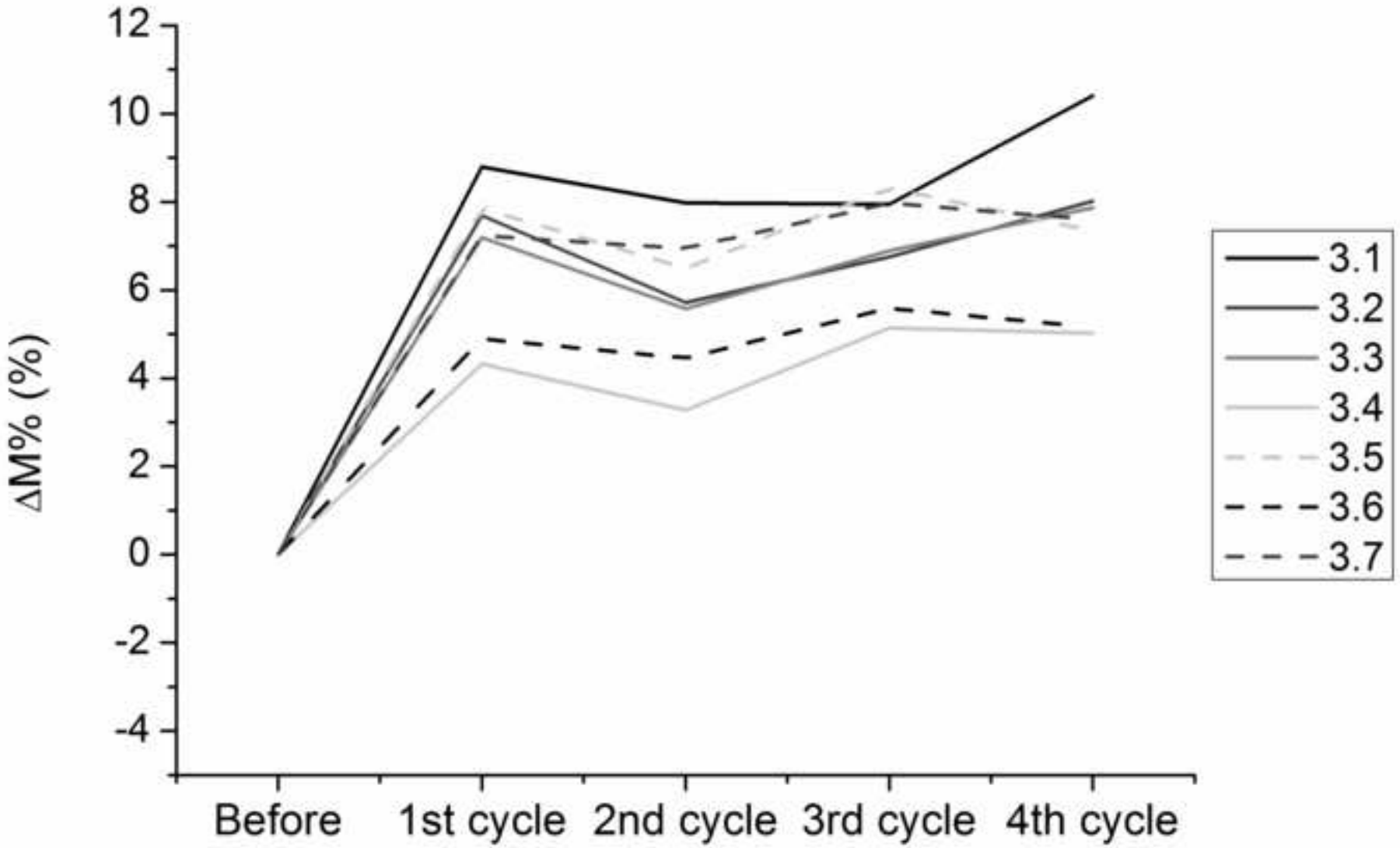

Figure 9

Click here to download high resolution image

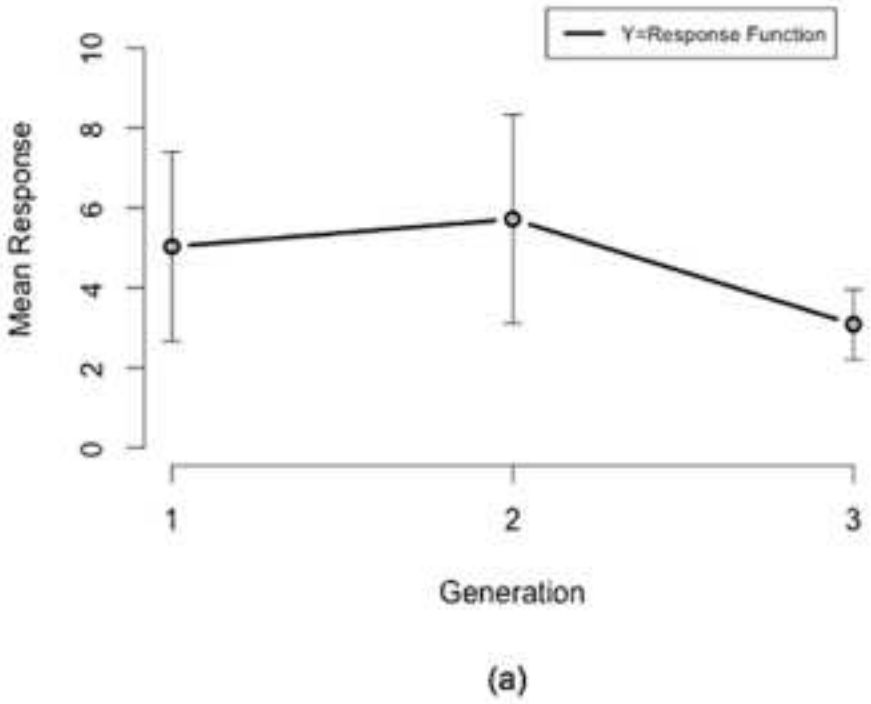

(a)

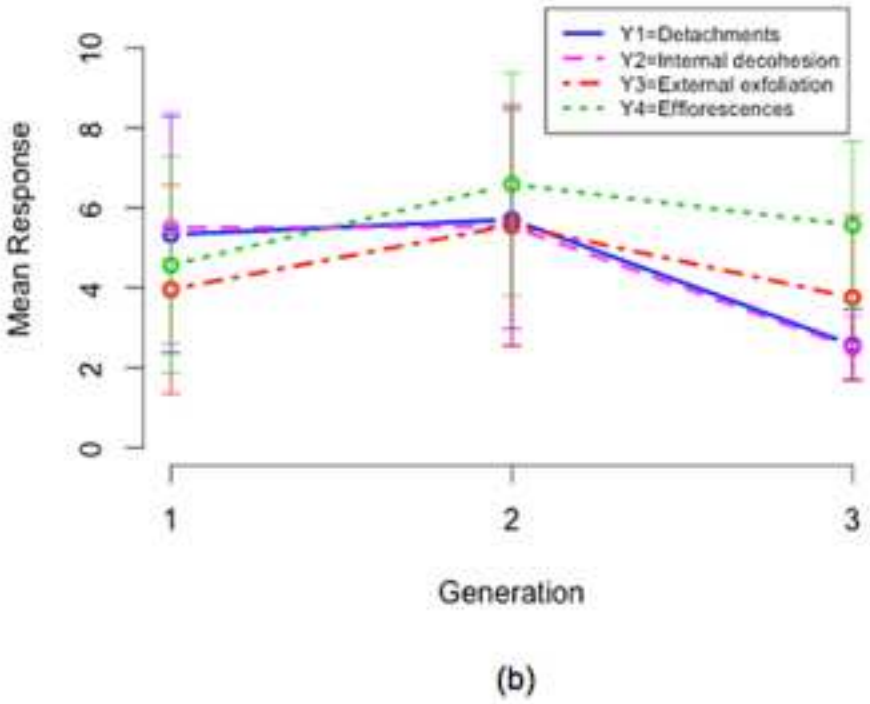

(b)

Figure 10

Click here to download high resolution image

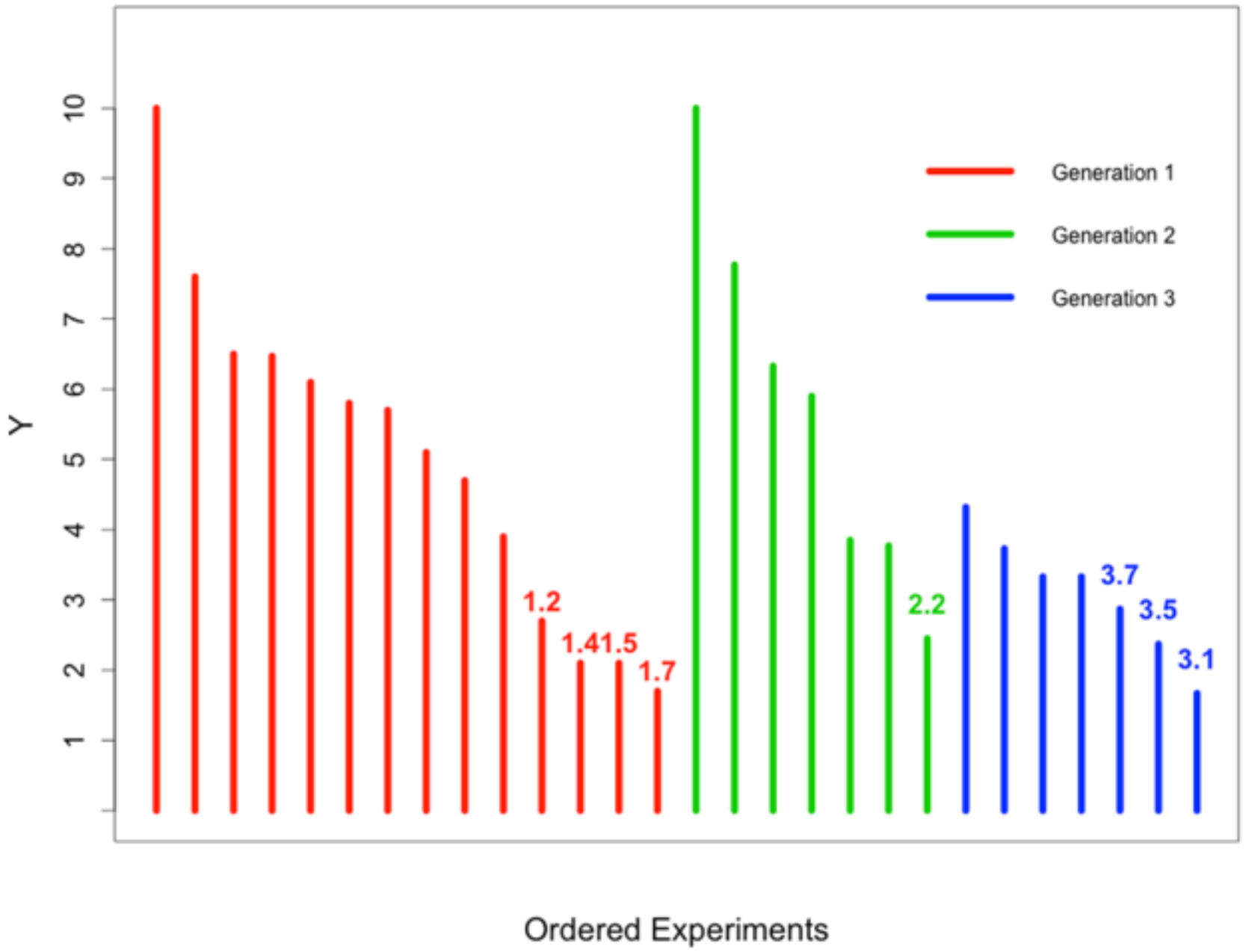

Figure 11
Click here to download high resolution image

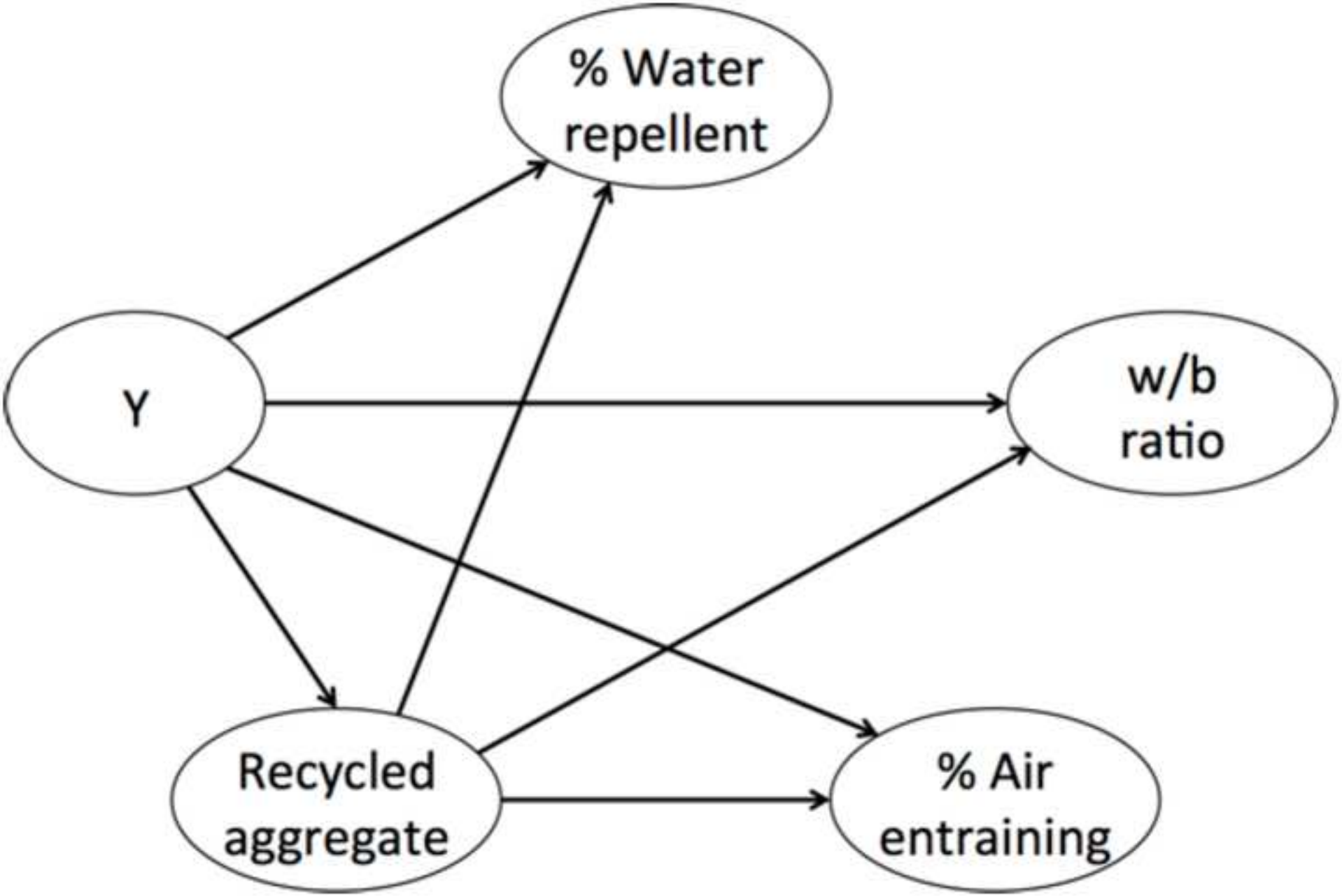

Figure 12

Click here to download high resolution image

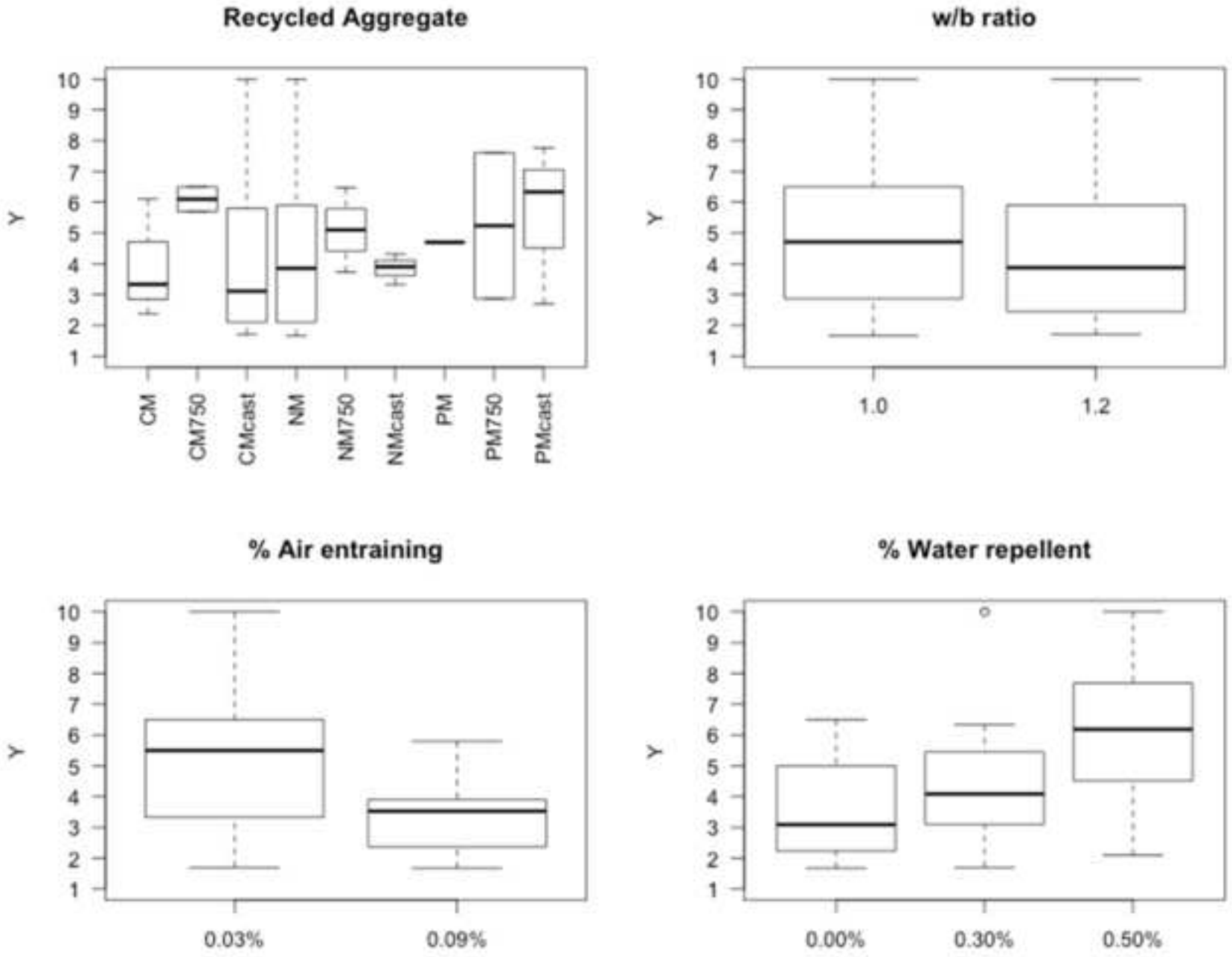

Figure 13
Click here to download high resolution image